signals

MDPI

Article

Internet of Spacecraft for Multi-Planetary Defense and Prosperity

Yiming Huo

Department of Electrical and Computer Engineering, University of Victoria, Victoria, BC V8P 5C2, Canada; yhuo@ieee.org

Abstract: Recent years have seen unprecedentedly fast-growing prosperity in the commercial space industry. Several privately funded aerospace manufacturers, such as Space Exploration Technologies Corporation (SpaceX) and Blue Origin have transformed what we used to know about this capital-intense industry and gradually reshaped the future of human civilization. As private spaceflight and multi-planetary immigration gradually become realities from science fiction (sci-fi) and theory, both opportunities and challenges will be presented. In this article, we first review the progress in space exploration and the underlying space technologies. Next, we revisit the K-Pg extinction event and the Chelyabinsk event and predict extra-terrestrialization, terraformation, and planetary defense, including the emerging near-Earth object (NEO) observation and NEO impact avoidance technologies and strategies. Furthermore, a framework for the Solar Communication and Defense Networks (SCADN) with advanced algorithms and high efficacy is proposed to enable an Internet of distributed deep-space sensing, communications, and defense to cope with disastrous incidents such as asteroid/comet impacts. Furthermore, perspectives on the legislation, management, and supervision of founding the proposed SCADN are also discussed in depth.

Keywords: space exploration; Internet of spacecraft; extra-terrestrialization; multi-planetary civilization; near-Earth object (NEO); Internet of distributed deep-space sensing; solar communication and defense network (SCADN); multi-planetary defense; space edge computing; space edge artificial intelligence (AI); legislation

check for updates

Citation: Huo, Y. Internet of Spacecraft for Multi-Planetary Defense and Prosperity. *Signals* **2022**, *3*, 428–467. https://doi.org/10.3390/signals3030026

Academic Editor: Manuel Duarte Ortigueira

Received: 10 May 2022
Accepted: 14 June 2022
Published: 22 June 2022

Publisher's Note: MDPI stays neutral with regard to jurisdictional claims in published maps and institutional affiliations.

Copyright: © 2022 by the author. Licensee MDPI, Basel, Switzerland. This article is an open access article distributed under the terms and conditions of the Creative Commons Attribution (CC BY) license (https://creativecommons.org/licenses/by/4.0/).

1. Introduction

Since the first artificial Earth satellite, Sputnik 1, was sent into an elliptical low Earth orbit (LEO) by the Soviet Union (USSR) on 4 October 1957, humans have opened a gate to the space age. Another historical milestone was carved by the National Aeronautics and Space Administration's (NASA) Apollo 11, the first crewed spacecraft to land humans on another celestial body, the Moon, on 20 July 1969 at 20:17 coordinated universal time (UTC). To date, tens of thousands of spacecraft have been sent to outer space which is defined by the von Karman line at 100 km above Earth's mean sea level. By the generalized definition, a spacecraft is a vehicle or machine designed to fly in outer space, and it can be categorized into two major types: crewed and uncrewed. As of 2021, only three nations have flown crewed spacecraft, the USSR/Russia, the USA, and China. The first crewed spacecraft, Vostok 1, was made by the Soviet Union and carried Soviet cosmonaut Yuri Gagarin into space in 1961, while the second crewed spacecraft named Freedom 7 was launched by United States, also in 1961, and carried the first American astronaut Alan Shepard, to an altitude of just over 187 km (km). On the other hand, uncrewed spacecraft include Earth-orbit satellites, lunar probes, planetary probes, asteroid/comet probes, and other deep-space probes. More details about examples of both crewed and uncrewed spacecraft launched are presented in Table 1.

Table 1. A summary of some crewed and uncrewed generalized spacecraft.

Category	Type	Example	Launch Year	Program Entity	Status	Feature
Crewed	spacecraft	Vostok 1	1961	USSR	retired	world's first
		Freedom 7	1961	USA	retired	reached 187 km
		Apollo 11 [1]	1969	USA	retired	world's first crewed moon landing; command and service module and lunar module
		Shenzhou 5	2003	China	retired	China's first
		Crew Dragon Resilience [2]	2020	USA (SpaceX)	ISS transportation mission finished	world's first crewed spaceflight operated by a commercial entity; reusable spacecraft
		Virgin Galactic Unity 22	2021	USA (Virgin Galactic)	continued	air-launched suborbital spaceplane for tourism; Mach 3.2 by rocket engine; reached 86.1 km
		New Shepard 4	2021	USA (Blue Origin)	continued	suborbital, reached 107.05 km; first flight with owner; reusable spacecraft
	space shuttle	Columbia	1981	USA	retired	reusable 23-ton payload
	space station	Salyut	1971	USSR	deorbited	world's first
		Skylab	1973	USA	deorbited	360 m^3, 2249 days
		Mir	1986	USSR/Russia	deorbited	350 m^3, 5511 days
		International Space Station (ISS) [3]	1998	USA/Russia/ ESA */ Canada/Japan	orbiting	915.6 m^3, largest area; longest service
		Tiangong-1	2011	China	deorbited	China's first prototype
		Tiangong	2021	China	orbiting	a space of 110 m^3
Uncrewed	Earth-orbit satellite	Sputnik 1	1957	USSR	deorbited	world's first artificial satellite
		Hubble Space Telescope (HST) [4]	1990	USA	orbiting	numerous scientific findings including research leading to Nobel Prizes
		Starlink	2019	USA (SpaceX)	orbiting	largest satellite constellation for broadband access
	lunar probe	Luna 1	1959	USSR	finished	world's first flyby
	solar probe	Parker Solar Probe	2018	USA	continued	the first to enter the solar atmosphere
	Mars probe	Mariner 4	1964	USA	finished	world's first flyby
		Perseverance	2020	USA	continued	Ingenuity, the first Mars robotic helicopter

Table 1. *Cont.*

Category	Type	Example	Launch Year	Program Entity	Status	Feature
		Voyager 1	1977	USA	traveling	first flybys of Jupiter, Saturn and Titan; Furthest and first interstellar spacecraft
	planetary probe	Cassini-Huygens [5]	1997	USA/ESA/ Italy	finished	first Saturn orbiter and moons flybys; Huygens probe landed on Titan, first (non-Earth) moon landing
		New Horizons	2006	USA	continued	first Pluto flyby
	comet probe	Rosetta [6]	2004	ESA	deorbited	first comet landing
	planetary defense	Double Asteroid Redirection Test (DART) [7]	2021	USA/ESA/ Italy/Japan	traveling	first kind for testing a method against near-Earth objects (NEO)

* the European Space Agency and it consists of 22 countries.

For the crewed spacecraft, governments played a key role initially. The Apollo 11 mission made a critical historic accomplishment of landing mankind for the first time on another celestial body in 1969. The first and biggest space station that has been collaboratively built and operated by several countries, the International Space Station (ISS), has been in service since 1998 and has been visited by 244 persons from 19 nations. The lunar module of Apollo 11 mission and the ISS are illustrated in Figure 1 (This file is in the public domain in the United States because it was solely created by NASA. NASA copyright policy states that "NASA material is not protected by copyright unless noted". NASA copyright policy also applies to some other images used in this paper). However, a noticeable trend in recent years is that the commercial space industry fueled by private capital has exponentially grown to accelerate technological transformation. One of the most influential corporations is Space Exploration Technologies Corp. (SpaceX) headquartered in Hawthorne, California. In 2015, SpaceX successfully launched and relanded a Falcon 9 rocket [8] and launched a returned Falcon 9 later in 2017, which paved a promising road to low-cost reusable launching vehicles. Moreover, SpaceX's Falcon 9 booster that launched the Crew-1 mission with the Crew Dragon Resilience in November 2020 is being reused for the Crew-2 mission, which is the first time the same rocket booster has been used for multiple human launches. The SpaceX Crew Dragon and Starship spacecraft are illustrated in Figure 2. Other non-governmental aerospace companies include California-based Virgin Galactic, which develops commercial spacecraft and provides suborbital spaceflights to space tourists, and Kent (Washington) headquartered Blue Origin, which also develops reusable launching vehicles and orbital technology.

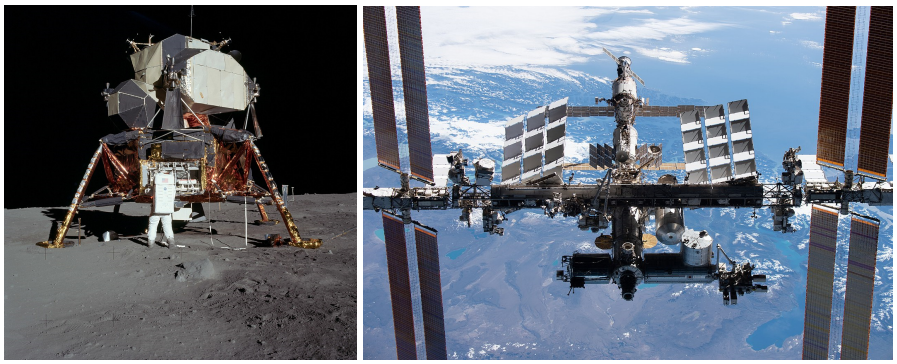

(**a**) (**b**)

Figure 1. (**a**) Apollo 11 lunar module Eagle and astronaut Buzz Aldrin on the Tranquility Base of the Moon on 20 July 1969 [1]; and (**b**) the view of ISS exterior and steelwork from the departing SpaceX Crew-2 spacecraft on 8 November 2021 [3].

(**a**) (**b**)

Figure 2. (**a**) The SpaceX Crew Dragon spacecraft docked to the ISS in 2021 [2]; and (**b**) Starship Serial Number (SN) 9 sitting on its launch pad in Starbase [9].

Furthermore, more uncrewed spacecraft have been launched, including various types such as Earth-orbit satellites, lunar/solar probes, planetary probes, comet probes, and asteroid probes (for planetary defense). The Hubble Space Telescope (HST) shown in Figure 3a is a space telescope launched into the LEO in 1990 and is still in operation. It features a 2.4-m mirror and is located at a variable altitude of around 537 to 540.9 km, with five main instruments to observe in the ultraviolet (UV), visible, and near-infrared regions of the electromagnetic spectrum. Many Hubble observations have led to breakthroughs in astrophysics [10,11], e.g., it assisted scientists to determine the expansion rate of the universe and resulted in the Nobel Prizes in 2011. Its end of mission is estimated to be around 2030–2040, while its successor, the James Webb Space Telescope (JWST) illustrated in Figure 3b was launched on 25 December 2021, and is supposed to be in the orbit of Sun–Earth L_2 [12,13], the second Lagrange point.

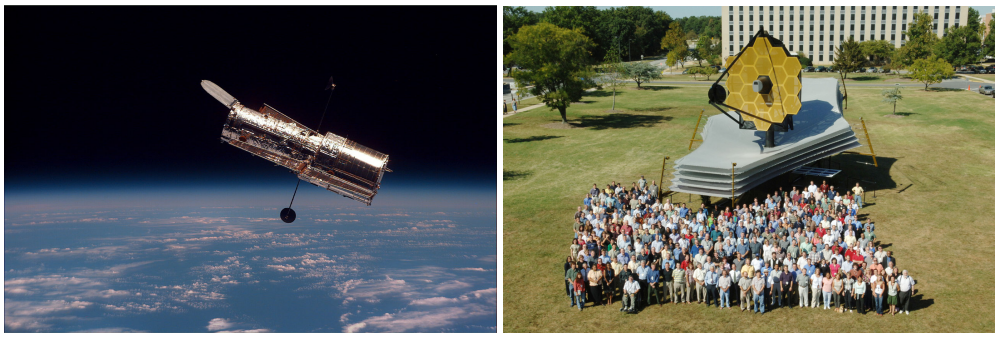

(**a**) (**b**)

Figure 3. (**a**) Hubble as seen from the Space Shuttle *Discovery* during its second servicing mission [4]; and (**b**) the James Webb Space Telescope full-scale model assembled on the lawn at Goddard Space Flight Center with the JWST team [14].

On the other hand, the planetary probes have been under the spotlight these years, and many nations have joined the race of sending probes to other planets. The recent operational Mars probes include Perseverance from the USA in 2020, Tianwen-1 from China, and Hope from the United Arab Emirates (UAE). One of the earliest pioneering spacecraft of this type is Voyager 1, launched in September 1977. As of November 2021, it has already traveled 155.5 astronomical units (AU) (23.26 billion km), which is currently out of the heliosphere and has become the first interstellar spacecraft and most distant artificial object from Earth.

The Cassini–Huygens spacecraft is a collaboration among NASA, the European Space Agency (ESA), and the Italian Space Agency (ASI) to study the planet Saturn and its system, including its rings and natural satellites. It consists of the Cassini space probe and ESA's Huygens lander, which landed on Saturn's largest moon, Titan, in January 2005. An illustration is presented in Figure 4a. NASA had conducted the mission extension after 2008 until September 2017 when Cassini was intentionally sent into Saturn's atmosphere to be destroyed to prevent biological contamination. Many astonishing scientific discoveries have been reported from its 20-year journey in space, which include the observation and analysis of Enceladus' water vapor plume [15,16] and tests of Albert Einstein's general theory of relativity [17].

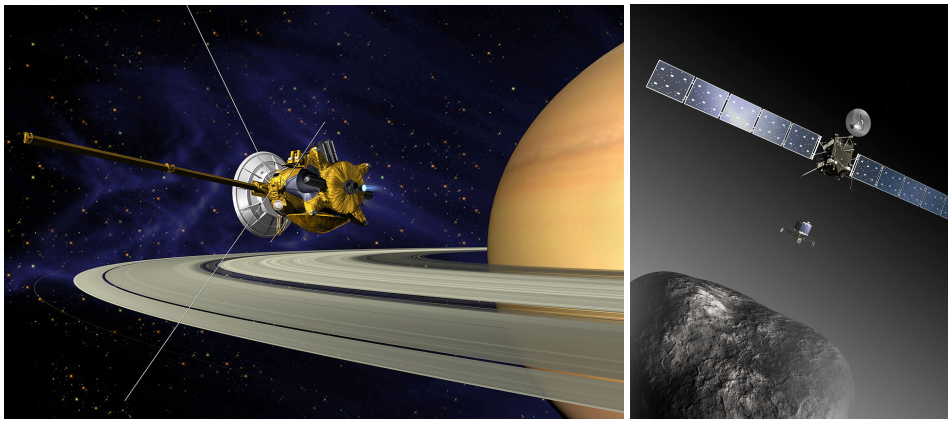

(**a**) (**b**)

Figure 4. (**a**) Illustration of an artist's concept of Cassini–Huygens' orbit insertion around Saturn [5]; and (**b**) artist's illustration of the Rosetta orbiter deploying the Philae lander to comet 67P/Churyumov–Gerasimenko [6].

In addition to the planetary probe, the comet probe is another type of spacecraft, and one representative is the Rosetta spacecraft designed and launched in March 2004 by ESA to study comet 67P [18]. It was the first spacecraft to orbit a comet nucleus and the first spacecraft to be in close proximity of a frozen comet toward a direction warmed by the Sun. The Rosetta orbiter dispatched the Philae lander for the first controlled touchdown on a comet nucleus. An illustration is shown in Figure 4b. The Philae's instruments obtained the first images from a comet's surface and made the first on-site analysis of its composition. On 30 September 2016, Rosetta was guided down to the comet's surface, and the mission ended on impact [19,20].

Moreover, on 24 November 2021, SpaceX Falcon 9 successfully launched the Double Asteroid Redirection Test (DART) spacecraft to test a method of planetary defense against near-Earth objects (NEOs) [7]. The DART spacecraft hosts no scientific payload, but it does include sensors and a navigation system and plans to arrive at 65,803 Didymos, a sub-kilometer asteroid and synchronous binary system classified as a potentially hazardous asteroid. Then, DART is set to crash into the asteroid system deliberately. The collision is scheduled in September/October 2022 when the impact of the 500 kg DART will target the center of Dimorphos, which is the minor-planet moon of 65,803 Didymos. The ASI's secondary spacecraft, called LICIACube (Light Italian CubeSat for Imaging of Asteroids), a small CubeSat, will ride on DART and then separate 10 days before impact to acquire images of the impact and ejecta as it drifts past the asteroid. The effects of the impact of DART will also be monitored from ground-based telescopes and radar.

In addition, a mission to 16-Psyche, which is a massive M-type asteroid with a mean diameter of 220 $\pm$ 3 km [21] that orbits the Sun in the main asteroid belt, was proposed to NASA in 2014. The concept of a robotic Psyche orbiter was proposed by a team led by Lindy Elkins-Tanton [22], at Arizona State University. They proposed to use the spacecraft to orbit Psyche for 20 months and study its topography, surface features, gravity, magnetism, and other characteristics since Pysche is the only metallic core-like body discovered so far. The mission's launch date was moved up to July 2022 from the original date in October 2023, targeting a more efficient trajectory with a Mars gravity assist in 2023 and arriving in 2026. On 28 February 2020, SpaceX won a USD 117 million contract from NASA to launch the Psyche spacecraft in July 2022.

Apart from the representative missions, either accomplished or ongoing, mentioned above, there are many other spacecraft and space missions under construction or planned. Generally, exploring and discovering more unknowns of the universe is one of the most fundamental drives of the space projects, which stems from the curiosity rooted in the human species. Moreover, the technical advances in the related areas of the space industry reduce the cost and enable some previous theories to become practical and commercial plans such as space tourism and extraterrestrial colonization. Nevertheless, along with the exciting opportunities in the space age come unprecedented challenges, some of which may even pose potential extinction-level disasters to the human species. In this article, we will continue to investigate critical space missions/projects focusing on space colonization, which will be followed by the review and analysis of the asteroid threat and planetary defense. To cope with the known challenges and difficulties, a novel framework and network based on the Internet of spacecraft is presented and analyzed. The novelties and contributions of this paper can be unfolded in several aspects as follows:

1. A comprehensive review of spacecraft projects, astronomical research, space exploration missions of critical milestones in human history is introduced and reviewed.
2. A thorough review, investigation, and analysis of the outer-space threats, planetary defense, and space colonization are presented. The theories and scientific findings of the origins of asteroids and comets plus the technologies of detection and mitigation of potentially hazardous objects are investigated and analyzed.
3. A novel framework named the Solar Communication and Defense Networks (SCADN) is proposed. It consists of a large number of distributed spacecraft/spaceships which are capable of enabling the Internet of distributed deep-space sensing, communica-

tions, and defense. An in-depth analysis is conducted to analyze how SCADN can increase the success rate of early detection of asteroids/comets/objects jeopardizing the safety of Earth and other colonized planets/moons. Furthermore, the SCADN-based mitigation strategies of preventing outer-space objects triggered extinction events are also presented and discussed.

4. Last but not least, to better serve the common interest of all mankind, several legal matters and legislative concerns about founding the SCADN framework have been presented and discussed.

The remainder of this paper is organized as follows. Section 2 reviews and analyzes current multi-planetary colonization projects and plans, with life's transition from sea to land and terraforming perspectives discussed. Section 3 presents a detailed review and in-depth analysis of the outer space threats and events, followed by a brief historical review of planetary defense. Section 4 further shows the state-of-the-art technologies of planetary defense. Section 5 proposes the concept of the SCADN framework to cope with potential space threats and discusses how the SCADN framework can mitigate them and facilitate extraterrestrial colonization. Eventually, Section 6 concludes this paper, and Section 7 gives the future research directions.

2. Extra-Terrestrialization: Make Life Multi-Planetary

It is generally believed that life on Earth began in the water and had been aquatic for billions of years. About 530 million years ago, sea creatures likely related to arthropods first began to make forays onto land [23]. Terrestrial invasion is one important milestone in the history of life [24], and the evolution of terrestrial vertebrates started around 385 million years ago. Authors in [25] have suggested from their data that a massive increase in visual range occurred prior to the subsequent evolution of fully terrestrial limbs as well as the emergence of elaborated action sequences through planning circuits in the nervous system. The eye size is almost tripled when comparing the tetrapods with digited limbs that evolved with early lobe-finned fish. From simulation results of examined animals viewing objects through water, the eye size increase provides a negligible increase in performance, while the eye size increase enables a large performance increase of viewing through the air. Therefore, the advance in the visual senses plays a crucial role in terrestriality.

Today, on one hand, mankind's sensory abilities in both microscopic and macroscopic scales have been constantly enhanced by technological advancements, and on the other hand, potential resources in outer space and other celestial bodies have driven humans to evolve into a spacefaring civilization [26,27], which can also increase the probability of mankind's survival and prosperity in the universe. We can perhaps call this transformation 'Extra-Terrestrialization' in the history of life.

2.1. Space Transportation

It has not been long since humankind learned how to combat gravity, and transportation between the Earth's ground and outer space is still expensive and challenging. The space industry has been conventionally a capital-intensive risky business [28]. The launch cost of the earliest launch vehicles such as the Vanguard rocket was $894,700 US dollars (USD) per kilogram when using the consumer price index (CPI) calculator to correct the cost to the reported date (in 2018) [29]. The figure below summarizes and illustrates more historical data [29,30] of launch costs dating back to 1957, with the CPI calculator used to correct the original data (in 2018) to the end of 2021.

As shown in Figure 5, the orange round dots indicate the launch costs to the LEO in USD per kilogram (USD/kg). The maximum and minimum costs are almost 1000 times separated due to technological advancements and productivity improvement. Another critical factor accelerating this disruption is the aforementioned private capital invested in the space industry in recent years. Since its first commercial mission in 2013, SpaceX has led the commercial launch service. One critical milestone was marked in 2015 when SpaceX

successfully launched and relanded its Falcon 9 rocket on the ground pad [8], which paved the road for the launch vehicles' reusability and even lower launch cost.

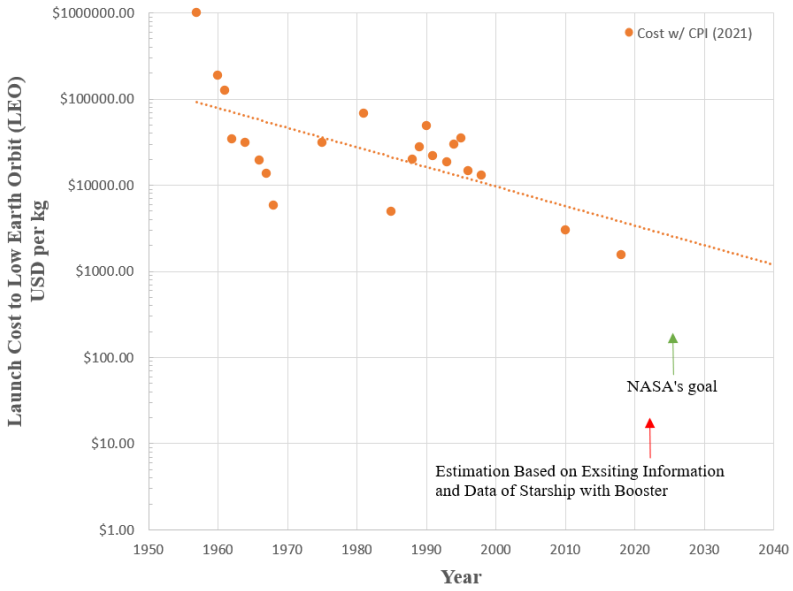

Figure 5. Low earth orbit launch cost change over time with 2021 CPI weighted.

A trend line based on existing available data indicates the general tendency of the cost change over a 60-year time period, which is a bit distant above the green triangular representing NASA's goal to bring the cost down to USD 100/pound or USD 220/kg in 2025 [31]. However, the scheduled first orbital flight of SpaceX's Starship that can deliver more than 100 tons (150 tons [26]) of payload to the LEO [32], might bend the trend line significantly downward in 2022. According to Elon Musk, the CEO and principal designer, the launch cost is estimated to be USD 2 million per launch [33], which can significantly reduce the cost to USD 20/kg.

However, the listed costs in the table are only for the launch reaching the LEO, while the trip to the Moon and Mars will cost significantly more. Take Falcon 9 for example, the mass of payload to LEO is 22.8 t and will be reduced to 8.3 t and 4 t for reaching a geosynchronous transfer orbit (GTO) and a Mars transfer orbit (MTO), respectively. Correspondingly, the cost of GTO and MTO will be 2.75 and 5.7 times higher than LEO. The reusability, large capacity, and advanced massive fabrication of launch vehicles could significantly lower the cost.

A payload comparison is summarized in [33], and it is worth mentioning that Big Falcon Rocket (BFR) was renamed after November 2018 by SpaceX, and the two-stage vehicle is technically composed of two parts, Starship (spacecraft) and the Super Heavy rocket (booster). As observed from the comparison in Figure 6, the Starship (with booster) is the most capable launch vehicle in human history and even outperforms SATURN V by >7%. All well-known rockets are presented and compared in height and payload.

Figure 6. Payload to LEO comparison of several worldwide launch vehicles, based on concept and data in [27].

2.2. An Interplanetary Spacecraft Design Example: Starship

Starship (without the booster) is 48-m long, and its dry mass is around 85 tons. The ship will contain 1100 tons of propellant with an ascent design of 150 tons and a return mass of 50 tons [27]. SpaceX has designed the engine section in the rear, the propellant tanks in the middle, and an eight-story tall payload bay in the front. In particular, the giant deep cryo-liquid oxygen tank made of carbon fiber is 1000 cubic meters of volume inside and more pressurized volume than an A380 airliner [27]. The delta wing at the back will enable Starship to handle the balancing challenges under various situations including zero/thin/dense atmosphere and/or with zero/low/heavy payload in the front [27]. Eventually, Starship can facilitate almost all types of entry/landing challenges in either a moon or a planet in the solar system.

Moreover, Starship (without booster) is expected to carry 240 tons of sub-cooled methane (CH) and 860 tons of oxygen as the propellant. The ship engine section consists of four vacuum Raptor engines and two sea-level engines, and all six engines are capable of gimbaling [27]. However, in another reference [27], the interplanetary spaceship is specified to have three sea-level engines with six vacuum engines. There might be more Starship design versions when the deployment and testing are carried out. Moreover, the booster, or Super Heavy rocket is equipped with 42 Raptor engines. The main body of the whole Starship including the Super Heavy rocket is currently made of SAE 304 L stainless steel thanks to its low cost, high melting point, strength at cryogenic temperature, and ease of manufacturing. The heat shield attached to the ship body is composed of thousands of black hexagon tiles that contain silica. By using hexagon tiles, hot plasma on atmospheric entry cannot accelerate through zigzag gaps, and the heat shield can withstand up to 1400 °C [34]. More importantly, they can be used many times without maintenance.

Furthermore, the Mars transit configuration (MTC) of Starship consists of 40 cabins that can hold more than 100 people per flight taking approximately 6 months (3 months in very good scenario [27]). In addition, Starship-MTC is expected to facilitate life-support and other requirements of a long interplanetary trip such as storage, entertainment, and solar-storm shelter which can resist a solar flare, which is the abrupt eruption of electromagnetic (EM) radiation in the Sun's atmosphere, and the resulting energetic protons that can pass through the human body, causing biochemical damage.

Take the Mars transportation for example, the system architecture and flow chart are illustrated in Figure 7 based on [26,27]. The Super Heavy rocket launches the crewed and/or uncrewed Starship spacecraft to the Earth orbit first, then is refilled by uncrewed Starship tankers that are already deployed in Earth orbit [26,27]. Refilling the propellant (liquid oxygen (O_2) and methane (CH_4)) in orbit is essential as it can maximize the spaceship payload on the trip to the final destination such as the Moon or Mars, which eventually

could reduce the vehicle size and cost by 5–10 times and increase the launch rate [26]. It is worth mentioning that by establishing a self-sustaining base on the Moon, Mars, or other celestial bodies, a large number of spacecraft, likely to be several thousand with tens of thousands refilling operations, will require many launches every day [27]. Then, the refilled Starships will continue the travel to Mars, while the tanker refill ships will return to Earth for refilling and the next launch.

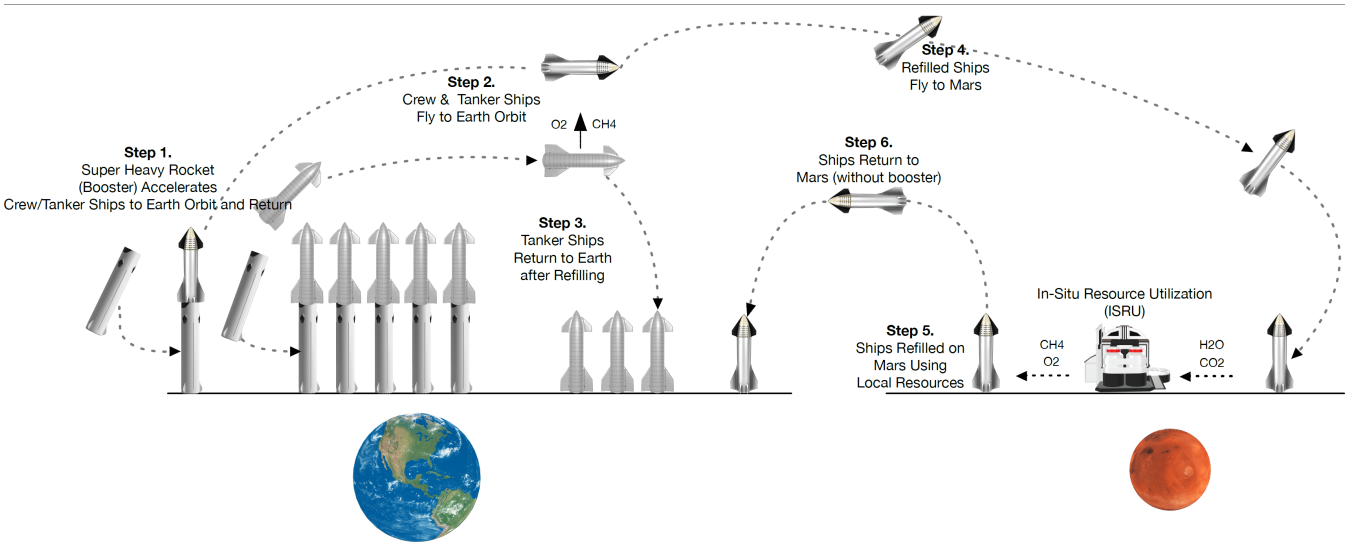

Figure 7. Illustration of Mars transit system architecture and flowchart, based on concept in [26].

2.3. Foundation on Another Celestial Body

Founding a human base or even a self-sustaining city on another celestial body is challenging in light of the current technological level [35]. Building the first colony for humankind on another celestial body with or without a thin atmosphere, with more severe damage from cosmic rays, solar radiation, or even asteroid impact, will have a challenging kickoff. Specifically, constructing reliable shelters either on the ground or underground is a huge mission requiring significant workforces and resources that depend on transportation at the very beginning. Take Mars, for example, 1 million people is a threshold required to maintain a civilization, which translates to at least 10,000 trips and 1000 ships [26]. Another challenge is the Earth–Mars rendezvous timing is roughly 26 months when the distance between two celestial bodies becomes periodically minimum, which means a huge number of preparation sand launches will occur in a very narrow time window, and the Mars fleet will have to depart en masse [26].

Compared to any other celestial body in the solar system, Mars is the most habitable telluric planet due to the suitable distance from the Sun and similar day length, land mass, and a bit less gravity (about 38% of Earth). The average Mars atmospheric pressure is about 600 Pa, or 0.5921% of Earth's standard atmosphere (ATM). Moreover, the Mars atmosphere is mainly composed of 95.32% CO_2, 2.7% N_2, 1.6% Ar, 0.13% O_2, etc. Moreover, billions of years ago, when Mars was warmer and the atmosphere was denser, channel-like valleys and riverbeds were highly likely to have emerged on the surface with flowing water [36–38].

However, due to the low temperature and atmospheric pressure today, liquid water cannot exist on the surface, although some water vapor is held in the atmosphere and some other liquid water might be released occasionally by the volcanic activity and asteroid impact. Most of the water on Mars is locked in the polar caps of which the larger one is the northern cap, Planum Boreum, with a dimension of 1000 km across and 1.2 km thick. Furthermore, the northern cap is composed of 90% of water ice and carbon dioxide (CO_2) ice that has a seasonal change observed by the Hubble space telescope [39]. The southern

cap (Planum Australe) has a thick base of water ice topped with an 8-m layer of (CO_2) ice. The southern cap is the only place where CO_2 ice persists on Mars' surface year-around.

The rich content of CO_2 and water ice on Mars can facilitate local mass production of propellant based on the Sabatier reaction process as shown in Figure 7. For oxygen and methane production, the Sabatier catalytic reactor (SR) and co-production/electrolysis are shown as follows [40,41]:

$$CO_2 + 4\,H_2 \longrightarrow CH_4 + 2\,H_2O\,(g) \quad -164\ \text{kJ mol}^{-1}\ (\text{at } 298\ \text{K}), \tag{1}$$

where ruthenium (Ru) is used as the catalyst under the temperature of 200–300 °C.

$$2\,H_2O_{(l)} \xrightarrow{\text{electrolysis}} 2\,H_{2(g)} + O_{2(g)}. \tag{2}$$

According to [40], every 1 kg of propellant made on the Moon or Mars saves 7.4 to 11.3 kg in the LEO. The Mars ISRU can significantly take advantage of atmospheric and soil resources and thus facilitate future Moon and Mars missions or even missions to other celestial bodies. On the other hand, the minerals contained in the Mars soil such as iron, aluminium, magnesium, silicon, titanium, etc., can be used for building self-sustaining cities and spacecraft. However, there are challenges such as how to operate the construction and mass production in extreme environments with extreme temperature, pressure, dust, cosmic rays radiation, low gravity, and micro-gravity.

Moreover, due to the major motivations of conducting scientific research, resource mining, and ISRU [42], the Earth's Moon can be another crewed base although it is much smaller than a planet and has only 16.5% gravity as Earth and no atmosphere. The Moon has water ice, oxygen (in iron-rich lunar minerals and glasses) [43], and abundant solar power and mineral resources such as iron, aluminum, magnesium, silicon, calcium, titanium, and rare-earth elements that are used for manufacturing electric vehicles, wind turbines, electronic devices, and clean energy technologies. More importantly, the Moon is estimated to contain more than 1 million tons of helium-3 (^{3}He) at the surface [44], which can be potentially harvested for nuclear fusion. Furthermore, building a Moon base requires reliable systems that can operate remotely and accumulate considerable experience launching trips to Mars [45] and even further celestial bodies. As illustrated in Figure 8, a large number of (wirelessly) connected spaceships enabled with AI and advanced telecommunication and computing capabilities can mitigate the cross-planets/moons missions' challenges and enable seamlessly cooperative transportation.

(**a**)

Figure 8. *Cont.*

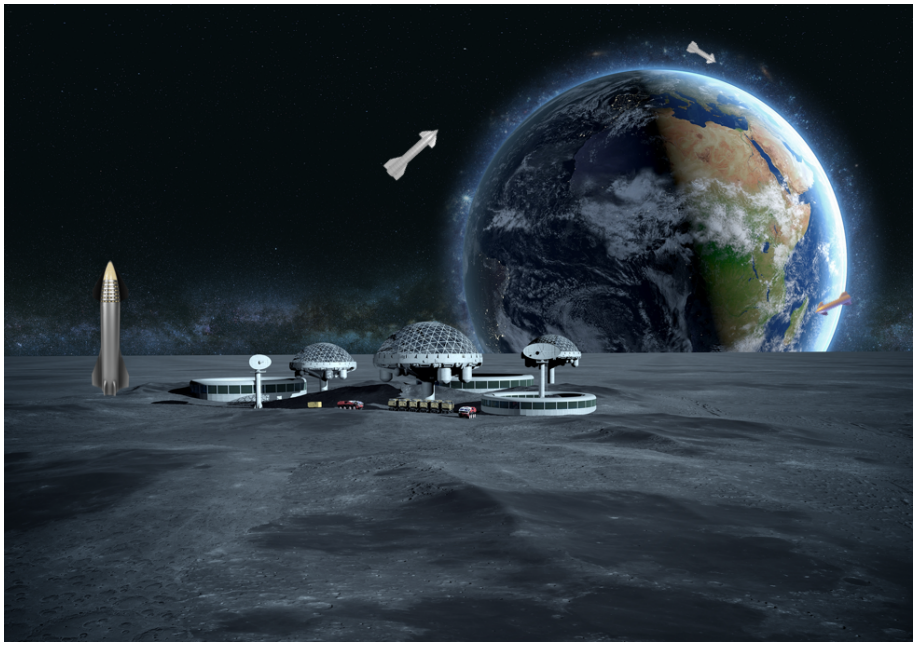

(**b**)

Figure 8. Illustration of foundation of: (**a**) Mars city; (**b**) Moon base with massive connected spaceships.

2.4. Terraforming

After setting the first foundation or even the first self-sustaining city with its own relatively comprehensive industry, agriculture, and services, terraforming, which is the hypothetical process of deliberately modifying the atmosphere, temperature, surface topography, or ecology of a celestial body to make it more similar or habitable to the environment of Earth, should commence. It can be a very long procedure but will benefit mankind and even Earth's animals and plants for the multi-planetary transition in the long term as depicted in Figure 9.

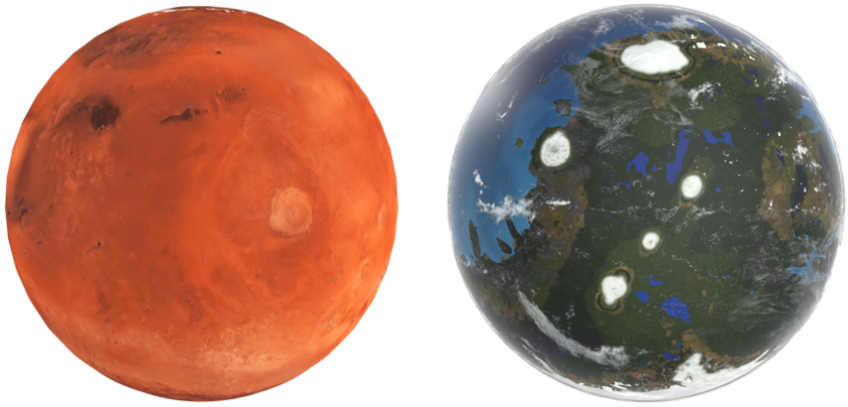

Figure 9. Illustration of Mars before and after terraforming.

In contrast to the controversy on terraforming Earth's Moon due to its higher difficulty [46,47], Mars is the most likely candidate to be terraformed. For example, it is believed that Mars used to be a warmer and wetter planet [37,38], with a thicker atmosphere but lost it during a course of hundreds of millions of years due to reasons still unclear [48]. Some likely mechanisms behind it could be related to the planetary surface absorption of greenhouse gases such as carbon dioxide, the lack of powerful magnetosphere around Mars due to the ceased dynamo function [49], or asteroid impacts that ejected the ancient Martian atmosphere into deep space [50]. However, there is evidence from the NASA MAVEN

mission that the Mars atmosphere was removed due mainly to coronal mass ejection events, but Mars still retains a level of magnetosphere covering approximately 40% of the surface rather than uniformly covering and protecting the atmosphere from solar wind [51].

Theoretically, terraforming Mars is the reverse procedure of how it lost the atmosphere and water. Among many proposals, including exploding nuclear devices on Mars [52], several are particularly worth mentioning. Greenhouse gases such as carbon dioxide can be generated on Mars through heating [53], to form CO_2 clouds to scatter infrared radiation and thus trap the incoming solar radiation [54]. Subsequently, the raised temperature can add more greenhouse gases to the atmosphere, and the two processes will augment each other and form a positive loop. Moreover, authors in [55] have demonstrated a 2–3 cm-thick layer of silica aerogel which will simultaneously transmit sufficient visible light for photosynthesis, block hazardous ultraviolet radiation and raise temperatures underneath it permanently to above the melting point of water without the need for any internal heat source. All experiments and modeling were under Martian environmental conditions. On the other hand, as motivated by the microorganisms' diverse roles in sustaining life on Earth, authors in [56] have proposed a framework for a new discussion based on the scientific implications of future terraforming such as avoiding accidentally distributing Earth's harmful microorganisms and genes to extraterrestrial areas and letting life stretch as a continuum connecting certain planetary bodies, with microbes doing the work of pioneer habitat conditioning. However, it requires many rigorous systematic, and controlled experimental studies with an ethical platform developed on Earth in advance.

Several other celestial bodies, such as Venus, and Mercury, have also been studied for terraforming. Still, Mars may be the most feasible one within mankind's technological capabilities, although the economic resources required can call for an enormous global joint effort in various aspects.

3. Space Threats and Planetary Defense History

3.1. Serious Threats from Outer Space

3.1.1. Cretaceous–Paleogene Extinction

Threats such as asteroids and comets from somewhere outside Earth can result in enormously catastrophic consequences. The Cretaceous–Paleogene (K–Pg) extinction event is also known as the Cretaceous–Tertiary (K–T) extinction; it was a sudden mass extinction of around 75% of the plant and animal species on Earth, which happened approximately 66 million years ago [57,58]. With the exception of some ectothermic species, no tetrapods weighing more than 25 kg survived. A large number of species were erased from Earth in the K–Pg extinction, and the best-known are the non-avian dinosaurs. Moreover, it destroyed numerous other terrestrial organisms such as mammals, birds [59], lizards and snakes [60], insects, plants, teleost fishes [61], pterosaurs, plesiosaurs, and mosasaurs [58].

The root cause of the K–Pg extinction event was originally proposed to have been the impact of a massive comet or asteroid 10 to 15 km wide about 66 million years ago by a team of scientists led by Nobel Prize-winning physicist Luis Alvarez and his son Walter. The impact hypothesis is also known as the Alvarez hypothesis and was supported by the discovery of the 180 km sized Chicxulub crater in the Gulf of Mexico's Yucatán Peninsula which was summarized in the 1991 publication of [62]. Moreover, authors in [63] have presented more conclusive evidence that the K–Pg boundary clay represented the debris (unusually high levels of the metal iridium) from an asteroid impact. Such a massive impact would have instantly led to devastating shock waves, a large heat pulse, and global tsunamis. Moreover, the release of enormous quantities of dust, debris, and gases would have resulted in a prolonged cooling of Earth's surface, low light levels, and ocean acidification that would have decimated primary producers including microscopic marine algae as well as those species reliant upon them [63].

In particular, there is broad consensus that the Chixculub impactor was an asteroid rather than a comet with a broadly accepted diameter of around 10 km. The impact released estimated energy of between 1.3×10^{24} and 5.8×10^{25} joules (1.3–58 yottajoules), or

21–921 billion Hiroshima A-bombs [64]. In 2013, authors with expertise in modeling nuclear winter published their research about the impact winter [65], which indicated that the entire terrestrial biosphere might have burned based on the amount of soot in the global debris layer. Supposedly, a global soot-cloud blocked the sun and created a long-term winter effect. More recently, in 2020, authors published the climate-modeling of the extinction event supporting the asteroid impact instead of volcanism [66]. However, the extinction also provided other opportunities to enable many groups to radiate. For example, mammals diversified in the Paleogene [67] and evolved new forms such as horses, whales, bats, and primates which made the emergency of the Homo sapiens possible.

3.1.2. Other Significant Events

In addition to the serious K–Pg extinction event, some other significant events in the more recent timeline are also believed to be related to a comet or asteroid. The Younger Dryas that happened around 12,900 to 11,700 years before the present (BP) [68] was a return to glacial conditions after the Late Glacial Interstadial (LGI), which temporarily reversed the gradual climatic warming after the Last Glacial Maximum (LGM) started fading around 20,000 BP. For example, within decades, a sudden decline of temperatures in Greenland by 4 to 10 °C took place [68]. It is hypothesized that an impact event occurred in North America around 12,900 BP and initiated the Younger Dryas (YD) cooling [69] that lasted for 1200 years and became one of the possible major causes of the Quaternary extinction. Nanodiamonds which are usually the high-temperature products during extraterrestrial collision [70] have been found at the Younger Dryas Boundary (YDB) in the northern hemisphere [71,72]. The catastrophic consequences of this impact, including the abrupt YD cooling, contributed to the late Pleistocene megafaunal extinction (e.g., woolly mammoth, saber-toothed predator), promoted human cultural changes, and resulted in immediate decline in some post-Clovis human populations [69].

When the timeline moves closer to the present, on the morning of 30 June 1908, an enormous explosion of around 12 megatons (of TNT) [73] (approximately 800 Hiroshima A-bombs) occurred near the Podkamennaya Tunguska River in what is now Krasnoyarsk Krai, Russia. An estimated 80 million trees over a forest area of 2150 km^2 were flattened [74] with three people possibly dead in the event as reported by witnesses [73]. The atmospheric explosion of a stony meteoroid with an estimated dimension of 50–60 m [75] happened at an altitude of around 5 to 10 km after entering Earth's atmosphere with a high speed of about 27 km/s [73,76]. The meteoroid is believed to have disintegrated and exploded at a similar altitude. Therefore, there is no impact crater. The sounds were accompanied by a shock wave that knocked people down and broke windows hundreds of kilometers away [73].

The explosion was registered at seismic stations across Eurasia, and air waves were detected in Germany, Denmark, Croatia, the United Kingdom, and Washington, D.C. [77]. Over the next few days, night skies in Asia and Europe were aglow [78]. Moreover, a Smithsonian Astrophysical Observatory program at the Mount Wilson Observatory in California observed a months-long decrease in atmospheric transparency and an increase in suspended dust particles [79]. The Tunguska event is the largest impact event on Earth in recorded history.

Within the last decade, the most significant meteor event happened on 15 February 2013 at about 03:20 UTC over the southern Urals region of Russia. An approximately 20 m-sized asteroid entered the atmosphere at a shallow 18.3 $\pm$ 0.4 degree angle with a speed relative to Earth of 19.16 $\pm$ 0.15 km per second [80]. According to the record, the meteor generated brighter light than the Sun and was visible as far as 100 km, and some eyewitnesses also felt intense heat from the fireball. Its peak radiation occurred at 29.7 $\pm$ 0.7-km. Then the fragmentation left a thermally emitting debris cloud in this period, the final burst of which occurred at 27.0-km altitude over Chelyabinsk Oblast. The Chelyabinsk meteor shone 30 times brighter than the Sun and had an energy equivalent to more than 500 kilotons of TNT [81,82] which is around 33.3 times the energy released from the Hiroshima A-bomb.

Furthermore, the object did not release all of its kinetic energy in the form of a blast wave as some 90 kilotons of TNT of the total energy was emitted as visible light according to NASA's Jet Propulsion Laboratory (JPL) [83]. The explosion resulted in injuries to about 1500 people (a large majority due to shattered glass) and damaged 7200 buildings in six cities across the region. It is the largest known natural object to have entered Earth's atmosphere since the 1908 Tunguska event, and the only meteor confirmed to have resulted in many injuries [84].

In [85], the authors pointed out that Chelyabinsk meteor's orbit was incredibly similar to the 2.2-km-diameter near-Earth asteroid 86039, which was first observed in 1999. The unusual similarity strongly suggests that the two bodies used to be part of the same object. According to the simulations, the asteroid spent 6 weeks before the impact within an elongation of 45-degrees from the Sun, which is a region of the sky giving no access to ground-based telescopes. In earlier times, the asteroid was always too faint to be observed [85]. Figure 10 illustrates and compares the sizes of the Chelyabink meteor, the Tunguska meteor, and the Barringer crater meteor [86].

Figure 10. Comparisons of approximate sizes of three notable impactors with New York Manhattan as the background.

3.2. Planetary Defense: When and How It Started

3.2.1. Timeline

As early as in a book published in 1964 [87], authors Dandridge M. Cole and Donald W. Cox mentioned the potential risks and dangers of planetoid impacts, both naturally and those that might be intentionally brought about with hostility. Moreover, they argued for categorizing the minor planets and developing the technologies to land on, deflect, or even capture planetoids. In 1967, students at MIT completed a design study called Project Icarus to prevent a hypothetical impact on Earth by asteroid 1566 Icarus [88] that received considerable publicity. Furthermore, a series of studies on historical impact events on Earth such as [79,89] in the 1980s led to a later program to map objects in the solar system which cross Earth's orbit and are large enough to cause serious damage if they collide with Earth.

In January 1992, NASA sponsored a near-earth-object interception workshop hosted by Los Alamos National Laboratory where the issues and challenges to cope with intercepting celestial bodies that could impact Earth were discussed [90]. Furthermore, a 1992 US congressional study produced a Spaceguard Survey Report, and it resulted in a 1994 mandate that NASA locate 90% of near-Earth asteroids larger than 1 km within 10 years [91]. The impact of a celestial body much larger than 1 km in diameter could lead to worldwide damage potentially including the extinction of the human species. The initial Spaceguard goal was achieved with a period slightly longer than 10 years. An extension to the project

required NASA to reduce the minimum diameter of a near-Earth object to 140 m and locate more than 90% of them by 2020 [92,93]. However, the new goal was not met even with a 10-fold increase in a NEO program budget [94]. As of April 2018, more than 8000 near-Earth asteroids of 140 m and larger had been spotted, while 17,000 such near-Earth asteroids were estimated to remain undetected. By 2019, the total number of discovered near-Earth asteroids of all sizes was more than 19,000 [95].

In particular, the NASA-funded Catalina Sky Survey (CSS) discovered over 1150 NEOs between 2005 and 2007 [96]. In 2005, the Catalina Station (near Tucson, Arizona) based CSS became the most prolific NEO survey and surpassed Lincoln Near-Earth Asteroid Research (LINEAR) in the total number of NEOs and potentially hazardous asteroids discovered. As of 2020, the Catalina Sky Survey (CSS) has discovered 47% of the total recorded NEOs, and the annual number has seen a steady growth [97].

3.2.2. Organization and Projects

On the other hand, in June 2015, NASA and the National Nuclear Security Administration of the U.S. Department of Energy officially formed joint cooperation [98]. Then in January 2016, NASA officially announced the establishment of the Planetary Defense Coordination Office (PDCO) which aimed at identifying, tracking, and warning about potentially hazardous NEOs that are larger than 30–50 m in diameter and coordinating an effective emergency response, studying and developing mitigation technologies and techniques [99]. PDCO has been involved in several key NASA missions, namely OSIRIS-REx, NEOWISE, NEO Surveyor, and DART which has been mentioned earlier.

OSIRIS-REx, which represents Origins, Spectral Interpretation, Resource Identification, Security, Regolith Explorer, is a mission operated by NASA to study asteroids and the solar system study and obtain a sample of at least 60 g from an asteroid [100]. OSIRIS-REx was launched in September 2016 and rendezvoused with the asteroid 101955 Bennu in December 2018 [101]. In October 2020, it successfully touched down on Bennu and collected a sample with a mass of more than 60 g and is expected to return to Earth in September 2023 [102].

Moreover, NEOWISE (Near-Earth Object Wide-field Infrared Survey Explorer) is a transferred and renamed mission re-activated from the NASA infrared astronomy space telescope in the Explorer program, WISE (Wide-field Infrared Survey Explorer) [103,104]. WISE was launched in December 2009 and placed in hibernation mode in February 2011 when it had already discovered thousands of minor planets, numerous star clusters, and Earth's first Trojan asteroid [105]. Since the reboot of NEOWISE, NASA has been working with the Jet Propulsion Laboratory to investigate NEO threat scenarios and expects to find suitable solutions to mitigate the impact.

Last but not least, the NEO Surveyor, which was formerly called the Near-Earth Object Camera (NEOCam) and then the NEO Surveillance Mission, is also a space-based infrared telescope intended to survey the solar system for potentially hazardous asteroids larger than 140 m [106]. The NEO Surveyor spacecraft will be working in the orbit of Sun–Earth L_1 [106,107], the first Lagrange point of Sun–Earth, so that it can take a closer look at the Sun and objects inside Earth's orbit [106,108]. As a successor to the NEOWISE mission, the NEO Surveyor mission was implemented by PDCO. In January 2021, NASA authorized the mission to proceed to the preliminary design phase with the JPL leading the development [106]. In terms of [109], the NEO Surveyor has used a 50-cm onboard telescope which is a bit larger than the 40-cm WISE telescope that has already successfully discovered 34,000 asteroids, including 135 NEOs. Its field of view is many times larger than WISE, enabling it to discover new NEOs with sizes as small as 30–50 m in diameter [109]. The detection improvement is largely accredited to new detector arrays (2048 × 2048 pixels and produce 82 Gb of data per day [110]) which have been modified to detect longer infrared wavelengths while being optimized for looking into cold space with excellent noise characteristics. Furthermore, the good infrared performance does not necessitate the

use of cryogenic fluid refrigeration. The detector can be passively cooled to 30 K. Thus, there will not be a performance degradation due to running out of coolant [110].

Finally, the seal of the PDCO, OSIRIS-REx (in launch configuration), an the artist's depiction of the WISE (NEOWISE) and NEO Surveyor are illustrated in Figure 11, respectively.

Figure 11. (**a**) The seal of NASA's Planetary Defense Coordination Office (PDCO) [111]; (**b**) OSIRIS-REx in launch configuration [112]; (**c**) artist's concept of the Wide-field Infrared Survey Explorer (WISE) spacecraft in its orbit around Earth [113]; (**d**) artist's illustration of the NEOCam (NEO Surveyor) space telescope [114].

4. Planetary Defense: State-of-the-Art

4.1. Origins of Asteroids and Comets

4.1.1. The Main Asteroid Belt

The asteroid belt is also called the main asteroid belt (MAB) or main belt, a torus-shaped region in the inner solar system located roughly between the orbits of Jupiter and Mars. It accommodates a large number of solid, irregularly shaped bodies, called asteroids or minor planets, as illustrated in Figure 12. With a total mass of approximately 4% of Earth's Moon, the asteroid belt is the smallest and innermost circumstellar disc in the solar system. Furthermore, about half of the mass of the asteroid belt stems from the four largest asteroids, namely, Ceres, Vesta, Pallas, and Hygiea [115], and Ceres is the only dwarf planet with a mean diameter of 939.4 km [116]. The main asteroid belt is believed to have formed from the very early-stage solar nebula as a group of planetesimals which are the smaller precursors of the protoplanets [117]. The gravitational perturbations from Jupiter, the most giant planet in the solar system, pervaded the protoplanets with such high orbital energy that prevented them from accreting into a planet [118].

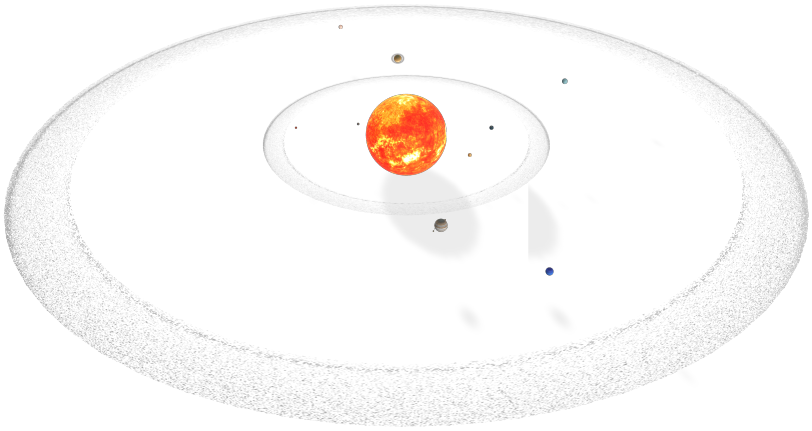

Figure 12. Illustration of the solar system with the main asteroid belt and the Kuiper belt [119].

The main asteroid belt is generally believed to be the source of most near-Earth objects. Authors in [120] have performed extensive orbital integrations for a representative set of main-belt things to locate escape routes into the near-Earth space. Their proposed method can identify all essential regions for NEOs and provide a specific distribution of asteroids that will enter the NEO regions. Moreover, another investigation [121] conducted by researchers from Europe and the United States discovered that approximately 470 million years ago, a 200 km sized asteroid was disrupted by a collision in the MAB, which generated many fragments into Earth's crossing orbits. During several millions of years following this significant cosmic catastrophic event, the meteorite production and cratering rate was significantly increased. For example, the 7.5 km wide Lockne crater in central Sweden is the consequence of the MAB event. Moreover, the authors provided evidence that the impact of a binary asteroid formed Lockne and its nearby companion, the 0.7 km diameter Målingen Crater [122].

Furthermore, the aforementioned Chelyabinsk asteroid is also considered to have an origin in the MAB. Based on the calculation of the pre-impact orbit of the Chelyabinsk asteroid and the orbit of asteroid 86039 (1999 NC43), researchers concluded that the pre-impact orbit is consistent with an origin in the MAB, most probably in the inner main belt near the v_6 secular resonance [85].

4.1.2. The Kuiper Belt

Comets, which are cosmic snowballs of frozen gases, rock, and dust, orbit the sun and have highly eccentric elliptical orbits with a wide range of orbital periods from several years to several million years. When passing close to the Sun, they are warmed up due to solar radiation and the solar wind and begin to release gases, which produce a visible atmosphere or coma, and sometimes also a tail. The tail can stretch away from the Sun for millions of miles [123]. As estimated, there are likely billions of comets orbiting the Sun in the Kuiper belt and in the even more distant Oort cloud.

There are two major categories of comets in terms of their orbital periods. Short-period comets are believed to originate in the Kuiper belt, which lies beyond the orbit of Neptune. As illustrated in Figure 12, the Kuiper belt is a donut-shaped region of icy bodies in the outer solar system [124], extending from the orbit of Neptune at approximately 30 AU to 55 AU from the Sun [124]. The Kuiper belt is similar to the MAB, but is much larger, around 20 times as wide and 20–200 times as massive [125]. It takes less than 200 years for short-period comets to orbit the Sun, usually the appearance of short-period comets is predictable since they have passed by before. The representative short-period comet is Halley's Comet, officially designated 1P/Halley and visible from Earth every 75–76 years.

Furthermore, long-period comets are believed to originate in the Oort cloud, which is a distant region of our solar system [126]. The Oort cloud is believed to be a giant spherical

shell surrounding the rest of the solar system. The inner edge is between 2000 and 5000 AU and the outer edge is 10,000 or even 100,000 AU (1.58 light years), which is one-quarter to halfway between the Sun and the nearest neighboring star system, Alpha Centauri (a triple star system 4.35 light years from Earth) [126]. The Oort Cloud might contain billions of objects, or even trillions of objects larger than 1 km [127]. Long-period comets move toward the Sun away from the Oort cloud due to gravitational perturbations caused by passing stars and the galactic tide. A typical example of long-period comets is Comet C/2013 A1 Siding Spring. It made a very close pass by Mars in 2014 and will not return to the inner Solar System for about 740,000 years [126].

On the one hand, comets bombarding the young Earth about four billion years ago brought vast quantities of water. Organic molecules, such as polycyclic aromatic hydrocarbons [128], have been found in comets, which has led to speculation that comets may have brought the critical precursors of life or even life itself to Earth. On the other hand, comets may have caused many significant events on Earth. There have been debates on whether an asteroid or a comet was responsible for the Chixulub impact [129]. Similar discussions or uncertainties on the impactor have also been seen in the investigation of the Tunguska event [130] and the Younger Dryas event [70].

It is important to mention humanity's first direct observation of an extraterrestrial collision of solar system objects, Comet Shoemaker–Levy 9's collision with Jupiter in July 1994. The comet, formally designated D/1993 F2, was discovered by astronomers Carolyn and Eugene Shoemaker and David Levy in 1993. By calculation, it may had been captured by Jupiter many years earlier and went through tidal breakup [131] in July 1992, eventually fragmenting and colliding with Jupiter in July 1994. This impact created a giant dark spot over 12,000 km (nearly one Earth diameter) across [132] and was estimated to have released an energy equivalent to 6,000,000 megatons of TNT (600 times the world's nuclear arsenal) [133].

In addition, the asteroid/comet may rarely come from neither the Kuiper belt nor the Oort cloud. 'Oumuamua is the first known interstellar object detected passing through the solar system. It was discovered by the Pan-STARRS telescope located at Haleakalā Observatory in Hawaii on 19 October 2017 when it was 0.22 AU from Earth and already passed its closest point to the Sun approximately 40 days later [134]. It was first classified as comet C/2017 U1 but reclassified again as asteroid A/2017 U1 due to the absence of a comet coma. Eventually, it was identified as 1I/2017 U1 because of its eligibility as an interstellar object. The authors conducted observation and verified a strongly hyperbolic trajectory in [135]. It has a hyperbolic excess velocity of 26.33 km/s (94,800 km/h), the speed relative to the Sun when traveling in interstellar space. In addition, there has been interesting discussion about its origin [136].

4.2. Potentially Hazardous Objects and Detection

According to [137], NEOs include asteroids and comets with perihelion distance q less than 1.3 AU, while near-Earth comets (NECs) are specifically restricted to only short-period comets with an orbital period of fewer than 200 years. Near-Earth asteroids (NEAs) consist of the majority of NEOs, which are categorized into four types, namely, Atira, Aten, Apollo, and Amor, according to their perihelion distance (q), aphelion distance (Q), and their semi-major axes (a). The definitions and relations of these four types are given and illustrated in Figure 13.

Furthermore, potentially hazardous objects (PHOs) are currently defined in terms of parameters that evaluate the asteroid's potential to make threatening close approaches to Earth [137]. For example, all objects with an Earth minimum orbit intersection distance (MOID) of 0.05 AU (7,480,000 km or 19.5 lunar distances) or less and an absolute magnitude (H) of 22.0 or less (equivalent to a diameter of at least 140 m) are considered PHOs. This dimension (140 m in diameter) is large enough to cause unprecedented regional devastation to human settlements in case of a land impact or a very dangerous tsunami in case of an ocean impact.

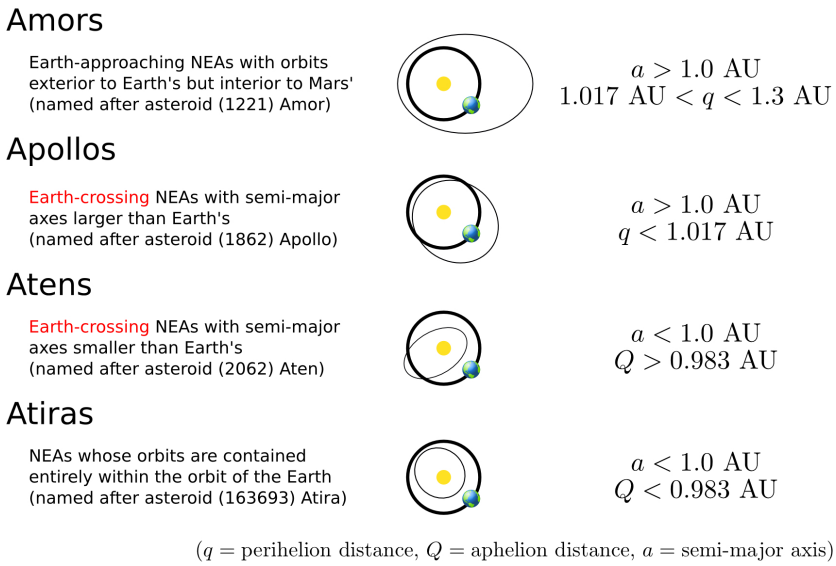

Figure 13. Four types of near-Earth asteroids known as Atira, Aten, Apollo, and Amor [137].

As of 1 May 2022, there are a total of 28,874 NEOs discovered and surveyed [138]. Only 117 (0.4%) of them are NECs, and the remaining are all NEAs. Furthermore, as illustrated in Figure 14, 10,070 of all NEAs are NEA-140 m (with diameters 140 m and larger), while 877 are NEA-km (with diameters 1 km and larger). Moreover, 2262 and 156 of all NEOs are categorized into PHA and PHA-km, respectively [138]. Eventually, the orbits of all known PHOs can be plotted for real-time tracking, such as in Figure 15.

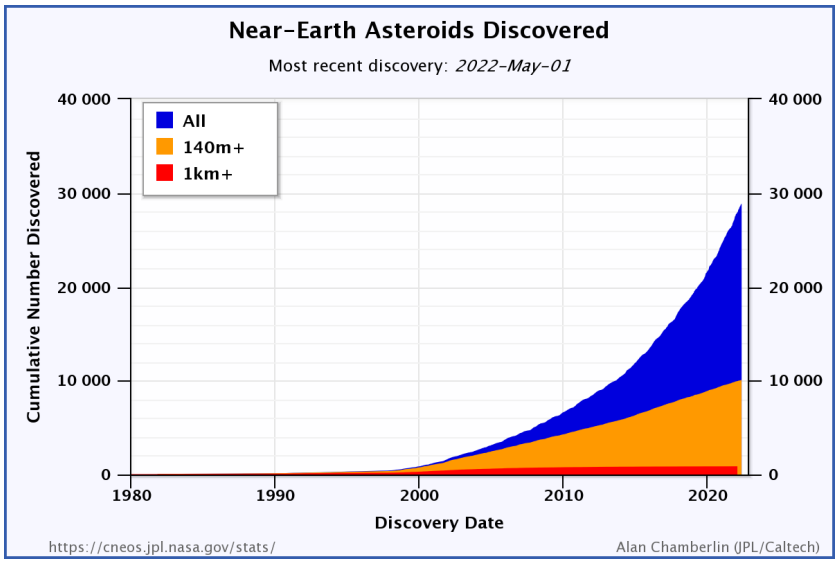

Figure 14. Near-Earth asteroids discovered as of 1 May 2022 [139].

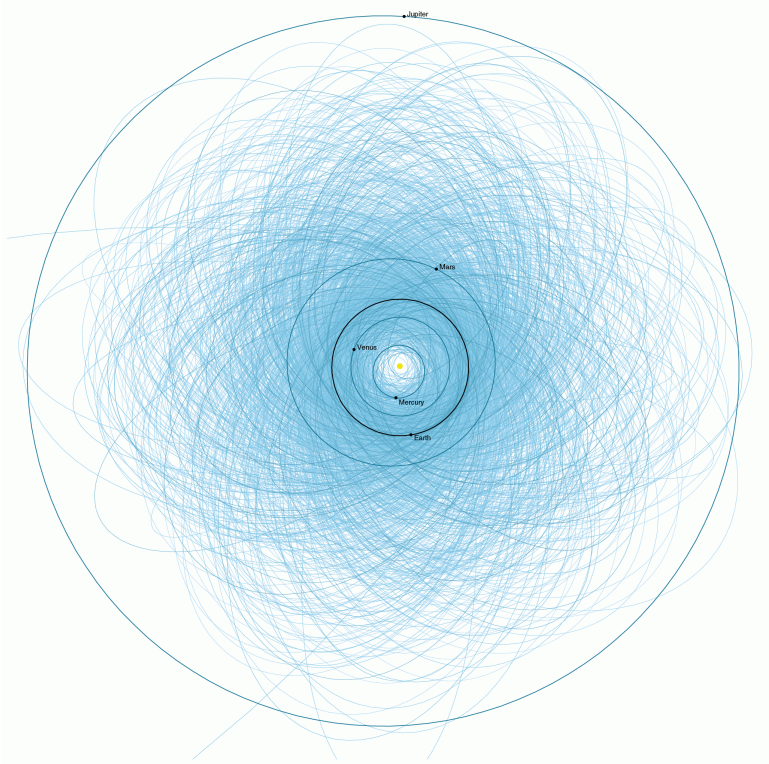

Figure 15. Plot of orbits of known potentially hazardous asteroids with sizes over 140 meters as of early 2013 [138].

In terms of theoretical estimations, impact events caused by PHOs in the 140-m and larger dimension may occur on average around once at least every 10,000 years, while a meteoroid the size of a football field hits Earth every 2000 years or so [140]. However, due to many uncertainties and factors, it is hard to predict when and where the impact will happen or if humanity will be ready to handle it. In addition, an impact event that is caused by PHOs smaller than 140 m and occurs in a shorter time period cannot be ignored since the aforementioned Tunguska event, and Chelyabinsk event were both caused by meteorites much smaller than 140 m. In fact, authors in [141] implied that 'Tunguska' impact rate on Earth is one event every 300 years and probably rather more frequently, which is much shorter than the current preferred value of 2000–3000 year.

4.3. State of the Art Space Objects Detection

4.3.1. Detection Capability According to Object Dimension

Prior to proposing any possible evolution plan for space object detection, it is noteworthy to review and conclude the performance of existing ones. The abovementioned Spaceguard survey activities involved several entities such as Lincoln Near-Earth Asteroid Research, Spacewatch, Near-Earth Asteroid Tracking (NEAT), Lowell Observatory Near-Earth-Object Search (LONEOS), Catalina Sky Survey, Campo Imperatore Near-Earth Object Survey (CINEOS), Japanese Spaceguard Association, Asiago-DLR Asteroid Survey (ADAS), and Near-Earth Object WISE. Thanks to the global joint efforts, most NEAs larger than 1 km in diameter (NEAs-km) have been surveyed and tracked. As of 2 May 2022, 877 NEAs-km have been discovered, which accounts for 95.3% of an estimated total of about 920 NEAs-km [142].

However, for NEAs with absolute magnitude $17.75 < H < 22.75$ (corresponding to a diameter larger than 100 m but smaller than 1 km), 12,058 have been surveyed as of 1 May 2022, which on average makes up only 15.8% of the estimated total ($(7 \pm 2) \times 10^4$) [142]. Based on the current detection pace, as shown in Figure 14, it might take decades to locate all these NEAs. Moreover, an even higher proportion of asteroids smaller than 100 m is

not yet located, which could take more resources and time to accomplish. This can also be interpreted that the current detection capability for asteroids of some specific dimension is still relatively limited, which could weaken the success rate of early warning and slow the reaction effort and mitigation deployment when a real threat appears.

4.3.2. Detection and Early Warning

Generally speaking, the current detection capability of NEOs is highly related to both the dimension and perihelio distances of NEOs. Theoretically, the smaller a NEO's dimension or perihelio is, the harder it can be to detect. The current detection system and detection range are mainly intended for near-Earth asteroids/comets with a maximum perihelio distance of 1.3 AU.

It will be more challenging to survey and locate non-NEO asteroids/comets such as in the MAB, the Kuiper belt, or even further regions of the solar system. However, these asteroids/comets can potentially become NEOs when a collision or gravitational disturbance flings them inward [143]. Authors in [120] have conducted an in-depth analysis of possible escape routes for asteroids to enter the near-Earth space.

On the other hand, there are possibly billions of comets that are orbiting the Sun and located in the Kuiper Belt and even more distant Oort Cloud. However, only 3743 of them so far have been discovered according to NASA [123]. The comets' orbits could be potentially altered due to gravitational disturbance, solar flare burst, collision, etc. As a result, it would not be a rare scenario for a comet to enter near-Earth space at high speed. 'Oumuamua is a typical case, and it was only 0.22 AU away from Earth when we discovered it [134]. Furthermore, it has been reported by NASA astronomers that 6 months' warning is not enough, and 5 to 10 years of preparation may be needed to stop an asteroid from hitting Earth based on the simulated exercise conducted by the 2021 Planetary Defense Conference [144]. Consequently, it will be critical and necessary to enhance the detection capability so that more preparation time could be obtained for humanity.

4.3.3. On-Ground Observatories

One of the possible and feasible strategies is to deploy more survey stations dedicated to discovering more asteroids/comets, which are not only categorized as NEOs but also are located in more distant regions. When reviewing the current near-Earth asteroid discoveries by survey, as illustrated in Figure 16, a majority of NEA discoveries have been made by Arizona-based Catalina and Hawaii-based Pan-STARRS since 2011. The Catalina Sky Survey uses three telescopes: a 1.5 m f/1.6 Cassegrain reflector telescope on the summit of Mount Lemmon (around 2791 m), a 68 cm f/ 1.7 Schmidt telescope near Mount Bigelow, and a 1-m f/2.6 follow-up telescope also on Mount Lemmon. Furthermore, the Panoramic Survey Telescope and Rapid Response System (Pan-STARRS) is located at Haleakalā Observatory, Hawaii, US, and consists of two 1.8 m Ritchey–Chrétien telescopes on the summit of Haleakalā (also known as East Maui Volcano) which has an elevation of 3055 m. The construction of both telescopes was funded by the U.S. Air Force and the NASA Near-Earth Object Observation Program. Both locations offer ideal observation conditions; for example, the air pollution and light pollution are minimal, the air density is significantly lower, the annual precipitation is extremely low, and the temperature fluctuation through the year is also very small. Furthermore, in astronomy, seeing refers to the degradation of the image of an astronomical object due to turbulent airflows in the atmosphere of Earth, and it may cause the blurring, twinkling, or variable distortion of the image. The Haleakalā observatory can also provide the best condition in terms of seeing. Another place providing such conditions is Roque de los Muchachos Observatory, located on the island of La Palma in the Canary Islands, Spain.

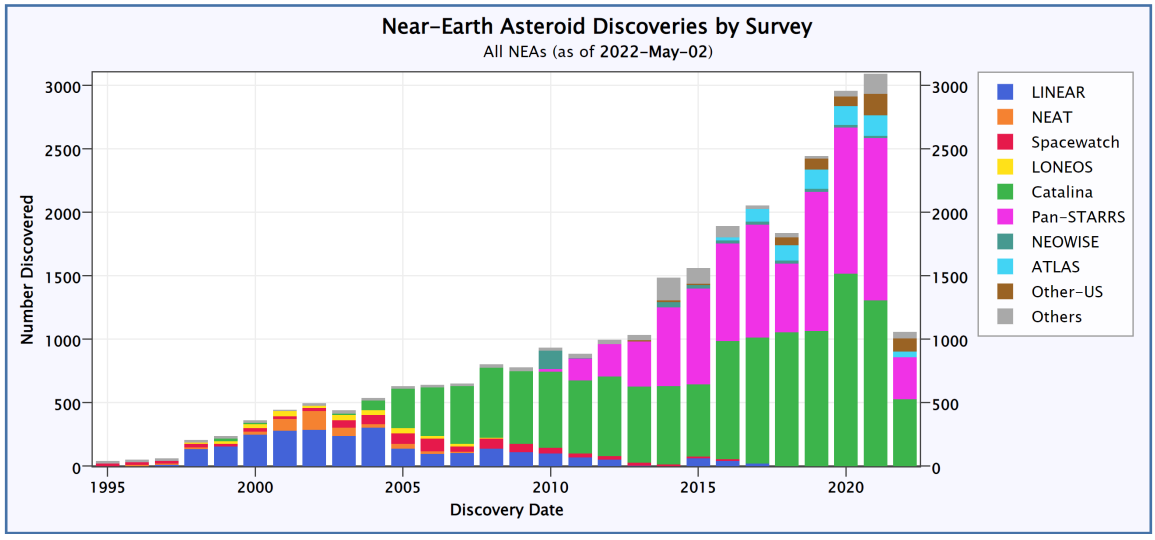

Figure 16. Plot of the number of NEA discoveries per year, by survey [139].

Therefore, finding ideal locations for ground observatories is challenging since many unique conditions need to be fulfilled. Moreover, when looking at the bigger picture, the ground observatories in the northern hemisphere or the southern hemisphere can only observe some portion of the entire sky. Joint efforts should be synchronized to thoroughly survey the entire sky in order not to miss any suspicious near-Earth object. In fact, the ideal place for founding observatories in the southern hemisphere is in the Atacama Desert, which is a desert plateau in northern Chile, covering a 1600 km strip of land on the Pacific coast, west of the Andes Mountains. The Atacama Desert has a high elevation and is the driest nonpolar desert globally, receiving less precipitation than the polar deserts. Due to its unique geological and weather conditions, some of its regions have been used for astronomical observatories and experimentation sites on Earth for Mars expedition simulations. The European Southern Observatory (ESO) operates three major observatories in the Atacama, which are known as, the La Silla Observatory, the Paranal Observatory, and the Llano de Chajnantor Observatory, and the ESO is currently building a fourth one, the Cerro Armazones Observatory, site of the future Extremely Large Telescope (ELT). The Llano de Chajnantor Observatory includes the famous Atacama Large Millimeter/submillimeter Array (ALMA), which is an astronomical interferometer of 66 radio telescopes and observes electromagnetic radiation at millimeter and submillimeter wavelengths. The array was constructed at the 5000 m elevation, which is crucial to reducing noise and decreasing signal attenuation due to Earth's atmosphere. However, these telescopes are not mainly dedicated to the NEO survey.

On the other hand, on-ground telescopes for the NEO survey mainly use radio frequencies and visible light. Only a few of them are infrared-based, such as the NASA Infrared Telescope Facility (NASA IRTF). Infrared telescopes hold some advantages, one of which is, for example, when observing in the near-infrared, the dust is transparent to it. Therefore, this explains why an optical telescope would be unable to see a star hidden in dust, whereas one working in the near-infrared would be able to detect its emission. Another advantage is that relatively cold objects invisible to optical telescopes become visible in the infrared. Interstellar gas, dust discs, asteroids, and brown dwarfs are all examples of objects that are too cold to shine in visible wavelengths but become conspicuous when viewed in the infrared [145]. Consequently, an infrared facilitated survey is beneficial for detecting asteroids/comets, which are usually cold and hard to discover. However, most infrared telescopes such as the Herschel, the NEOWISE, and the JWST, are placed in space to completely eliminate the interference from the Earth's atmosphere. Furthermore, cryogenic technology will be needed with spaceborne infrared detection since the low temperature can effectively suppress the detection of dark currents and background noise [146].

Moreover, from the radio astronomy perspective, powerful ground-based radio telescopes can effectively detect NEOs. For example, the California-based Goldstone Deep Space Communications Complex (GDSCC) made a historic observation of the 1000th near-Earth asteroid [147] on 22 August 2021 on its Deep Space Station (DSS) 14: "Mars" where an enormous Cassegrain antenna of 70-m diameter is installed. When created by the JPL to support the Pioneer program of deep space exploration probes, the location of the Goldstone complex was chosen to be in the Mojave Desert, distant from radio interference. The GDSCC was mainly intended for the vital two-way communications link that tracks and controls interplanetary spacecraft. However, it can also be used as high-sensitivity radio telescopes for astronomical research, such as radar mapping planets, asteroids, and comets.

Furthermore, the advances in astronomical spectroscopy also provide better measurement of the spectrum of electromagnetic radiation from celestial bodies. Scientists could detect molecules of interesting materials on celestial bodies and better understand the solar system's evolution. For example, a semiconfocal cavity coupled pulse echo spectrometer system designed in 65-nm CMOS is able to detect Nitrous Oxide (N_2O) that re-emits at 100.4917 GHz [148]. Furthermore, a 180-GHz pulsed CMOS transmitter with a high output power of 0.6 mW is presented for emission-based molecular detection [149]. It is predicted by Dr. Tang that the emission spectroscopy will play a crucial role in analyzing a plume or gas emission of a celestial body and be used in radio-astronomy looking at distant stellar objects. Therefore, emission spectroscopy can also be utilized to conduct precise spectroscopic analysis of the asteroids that are currently classified into three major types according to their spectra. In the former Tholen classification, the C-types are made of carbonaceous material, S-types consist mainly of silicates, and X-types are metallic. Then in 2002, the Tholen classification was upgraded into the SMASS classification, expanding the number of categories from 14 to 26 [150].

5. Multi-Planetary Detection, Communications, and Defense: Live Long and Prosper

At this point, we can summarize several key points from previous investigations as follows:

- First, due to many types of random events and their consequences, asteroids and comets can escape or change their former orbits and enter the near-Earth space, which increases the probability of their impact with Earth. The current asteroids/comets detection is focused on the NEO category, which may limit the preparation time allowed for humanity. Although more than 96% of total estimated large asteroids (with a diameter of 1 km and more) in the near-Earth space have been surveyed so far, the proportion of NEAs (with a diameter between 100 m and 1000 m) is still very low.
- Second, the detection capability of on-ground telescopes highly depends on their geological and meteorological conditions. Only several specific locations on Earth can fulfill such challenging requirements for high-quality observation. Moreover, most on-ground observatories operate in visible light and radio frequencies. Just a few ground-based telescopes work in infrared wavelengths, and many infrared telescopes are space-based to minimize the Earth's interference and background noise.
- Third, the ground-based observatories are usually powerful with abundant facilities and local technical support, while space-based ones normally depend only on the solar array and remote debugging. On the other hand, space-based telescopes have obvious advantages over the on-ground ones to survey the sky in infrared wavelengths, thus playing a crucial role in identifying and locating NEOs. For example, most asteroids are black, and small ones are difficult to see in the blackness of outer space with an optical telescope. Still, a telescope operating at infrared wavelengths is sensitive to asteroids' surfaces warmed by the Sun.

5.1. Evolving the Networks of Survey Stations

Based on the features and characteristics of asteroids/comets and related detection technologies, building and deploying more space-based survey stations with multiple techniques can accelerate the discovery of all potentially hazardous objects (PHOs). Furthermore, with minimal interference from Earth, space-based telescopes and spacecraft can more effectively survey the universe, with access to the full sky when deployed properly. In addition, the space-based survey stations are connected with on-ground stations and resources to form a more comprehensive and reliable network for PHOs detection. Next, we propose a framework for solar communication and defense networks (SCADN) which consists of the following critical components:

1. A large number of survey stations (on spacecraft) will be deployed into various orbits across the entire solar system to form an enormous Internet of spacecraft (IoS) networks. As humans are supposed to become a multi-planetary species after extra-terrestrialization, the colonization of other celestial bodies could also fall victim to asteroid/comets impact. For example, due to the lack of a thick atmosphere as on Earth, Mars could be more vulnerable to the impact of near-Mars objects (NMO). Moreover, Jupiter and Saturn, the gas giants which are 318 times and 95 times as massive as Earth, can affect and steer some asteroids away from Earth, thus providing some protection to humanity. However, Jupiter and Saturn attract asteroids/comets to their regions and increase the impact probability on their moons including Europa [151], Titan [152], and Enceladus [15] which are particularly interesting and may be possible sites for human colonization. Similarly, some moons of ice giants Uranus and Neptune also can serve as humanity's colonization and outpost for even further expeditions in the universe. Consequently, deploying survey stations and spacecraft into regions/orbits of Mars, Jupiter, Saturn, Uranus, and Neptune is also crucial.
2. As illustrated in Figure 17, for each planet in the solar system, multiple survey stations/spacecraft are deployed in the planet's orbit. In the SCADN, the specific locations for accommodating these spacecraft can be on Lagrange points where the gravitational forces of the two large bodies and the centrifugal force balance each other so that spacecraft only require minimal orbital corrections. Take Earth for example; multiple survey stations/spacecraft can be deployed on Earth–Sun Lagrange points, $L_{2,\,S\text{-}E}$, $L_{3,\,S\text{-}E}$, $L_{4,\,S\text{-}E}$, and $L_{5,\,S\text{-}E}$, respectively. There are several features enabled by adopting such a strategy. First, $L_{2,\,S\text{-}E}$, which has a distance of around 0.01 AU from Earth, can enable a high-performance survey (with minimal interference from the Sun) to the space in the direction away from the Sun but a reliable communication with Earth. Second, $L_{3,\,S\text{-}E}$, $L_{4,\,S\text{-}E}$, and $L_{5,\,S\text{-}E}$ can help survey space more thoroughly and completely than on/near-Earth stations. For instance, the object within a specific elongation from the Sun, which is a region of the sky giving no access to ground-based telescopes, will be discovered by stations deployed in these locations. Therefore, the probability of failed detection and the absence of alarms of incoming objects from outer space (such as the Chelyabinsk meteorite) will be minimized.
3. Furthermore, as shown in the exemplary illustration, the Lagrange points of other planets such as Venus, Mars, Jupiter, and Saturn, will also be deployed with survey stations/spacecraft. For example, Venus has an average distance of 0.72 AU from the Sun and orbits the Sun faster than other outer planets. Therefore, deploying survey stations/spacecraft into the four Lagrange points of Venus can also help survey the potentially hazardous objects approaching other outer planets (of Venus) more effectively. Since the space increases over the growth of orbits, deploying more survey stations/spacecraft for planets of interest using this method will cover more space and further minimize the failure detection and warning. It is noteworthy that Figure 17 is just such an exemplary case of many; Mercury, Uranus, and Neptune are not shown for simplicity. All survey stations and spacecraft are inter-connected and can collaborate on a series of survey tasks to realize a better overall performance gain. On each Lagrange point, there may be more than one survey station/spacecraft

needed to fulfill the specific requirement. Eventually, a very large sphere of at least more than 30 AU in the radius can be covered under the SCADN so that many more space objects that previously could not be located/tracked by humans could be fully available in the database. Moreover, these survey stations/spacecraft could serve for other space exploration and scientific experiment tasks, thanks to their unique celestial coordinates.

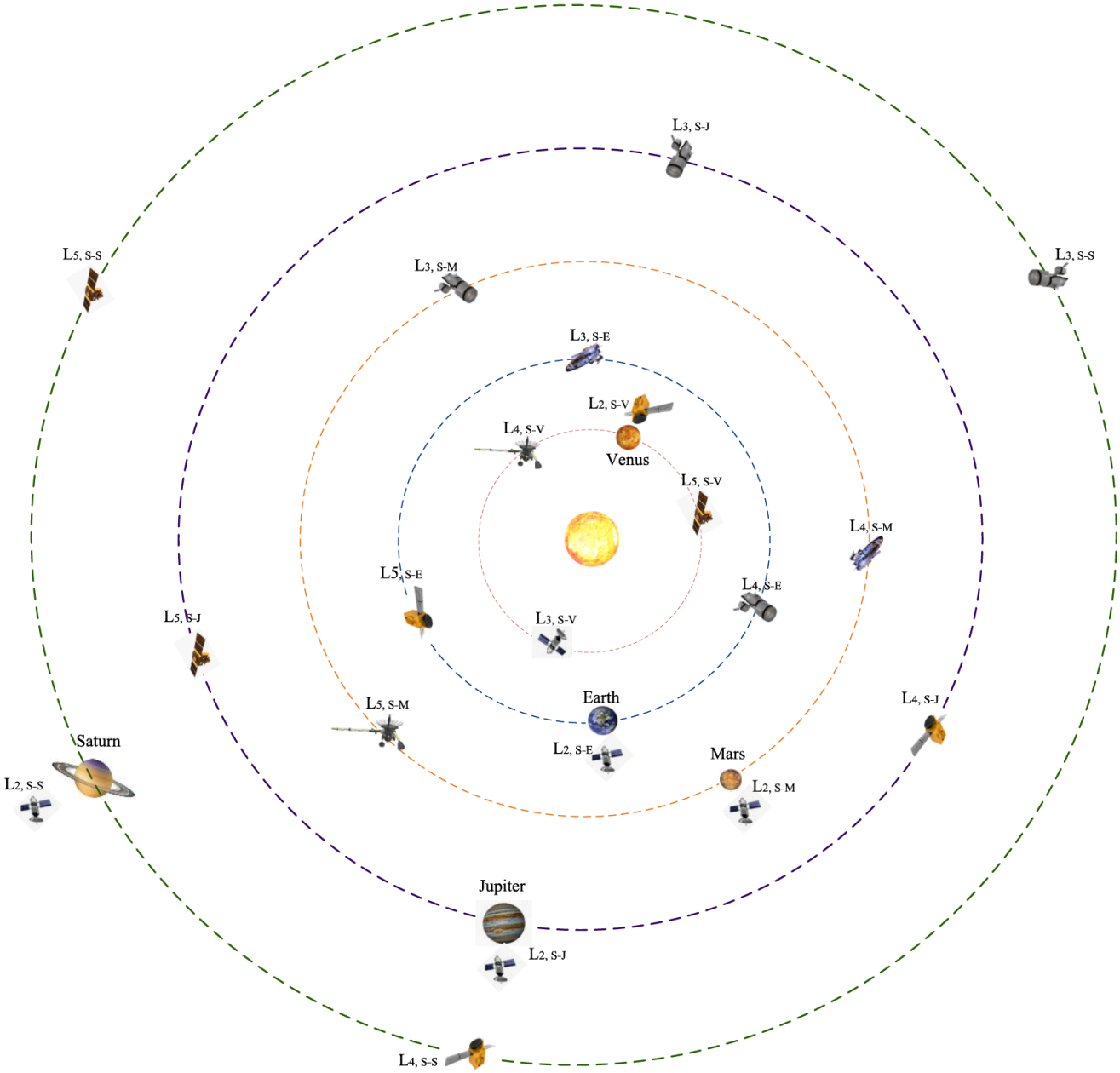

Figure 17. An exemplary illustration of survey stations and spacecraft deployed under the SCADN framework; in particular, the survey stations/spacecraft are deployed at Lagrange points of the solar planets (dimensions of orbits, planets and spacecraft are not scaled).

4. All survey stations and spacecraft are expected to communicate and connect with each other using multiple state-of-the-art communications and networking technologies. Some of the unprecedented challenges for wireless communications are the very long distances over which the wireless signals need to travel and the solar flares that can seriously interrupt the radio communication. In addition, the meteorological

conditions on Earth and other celestial bodies can lead to degradation in wireless communications. Although the low data rate communication over very long distances in deep space is proven to be working well (such as Voyager 1 and 2 that are currently around 155.6 AU and 129.9 AU from the Sun), a high data rate can still be challenging even today. Another challenge is the significant latency. With 1 AU distance meaning 499 s for light to travel in free space, the distance between Saturn's $L_{3,\,S\text{-}S}$ and Saturn itself is 19 AU or 9481 s (around 158 min) for light to fly. The communication latency between Neptune and its $L_{3,\,S\text{-}N}$ is around 500 min. Moreover, the latency between Earth and Lagrange points of different planets varies over time.

5. Considering the challenges of wireless communications over extremely long propagation, particularly the very large latency, using Earth as the only routing point to store, exchange, and process data and telemetry commands from survey stations/spacecraft may lead to a very long latency and low efficiency. There are several potential solutions to this dilemma. For example, it would be beneficial to enable artificial intelligence (AI) and edge computing on the survey stations/spacecraft so that they could process the image and data extracted from space and determine if any detection falls into interest or any further resource (other survey stations/spacecraft and computing power) is needed to assist in the task. Moreover, any communication interruption due to interference could be mitigated when using some of the available survey stations/spacecraft as relays. Eventually, such an AI and edge computing assisted, cell-free architect can improve the overall system efficiency of wireless communications in deep space and identify the objects of interest.
6. Such a multi-task capable SCADN framework can facilitate more interesting space exploration missions and astronomical research. For example, the survey stations within the framework can be used to search for and observe exoplanets and black holes. The spacecraft/spaceships can even be dispatched to investigate any space object of interest in their vicinity so that some mysterious or strange objects (e.g., 'Oumuamua) and their origins could be better understood.

5.2. Equipping the SCADN with Mitigation Technologies

On top of the initial development and deployment of the SCADN, some further proactive strategies of mitigation can be utilized to reduce the probability of catastrophic consequences of the impact of space objects. Conventionally speaking, the mitigation techniques, or collision avoidance techniques, are developed based on metrics such as technology readiness, failure risks, operation feasibility, performance, and cost [153]. There have been various methods proposed to change the course of an asteroid or comet [154], which can be categorized by various types of attributes such as the type of mitigation, approach strategy, and energy source, as summarized and concluded in Table 2.

As observed, the energy source of the nuclear explosive device can provide the most effective approach to cope with PHOs of various sizes for either short-notice or long-notice threats, particularly against solid objects. However, many NEOs are believed to be loosely held together by gravity as "flying rubble piles" and thus cannot be effectively handled by the method of kinetic impactors or nuclear explosive devices. The indirect methods such as gravity tractor, focused solar energy, laser ablation, and ion beam shepherd might take more time to alter the PHO's trajectory but require early development and deployment, such as traveling to the PHO's proximity in advance, for the space rendezvous. Furthermore, the PHO deflection means of gravity tractor and focused solar energy and the deployment procedure of the DART mission are illustrated in the following Figure 18, respectively.

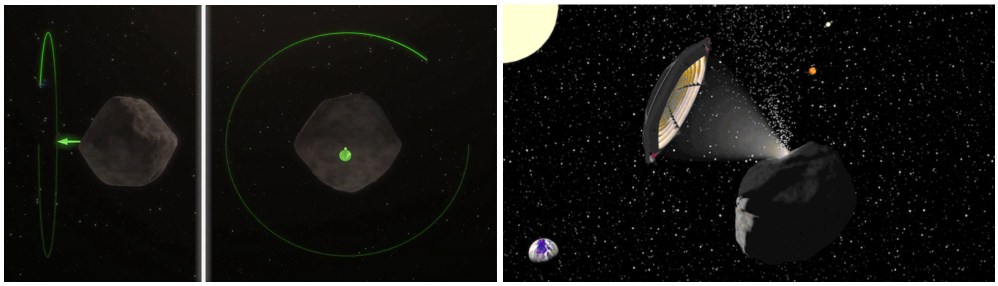

(**a**) (**b**)

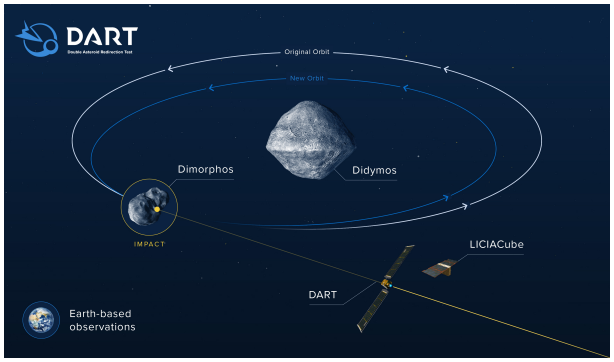

(**c**)

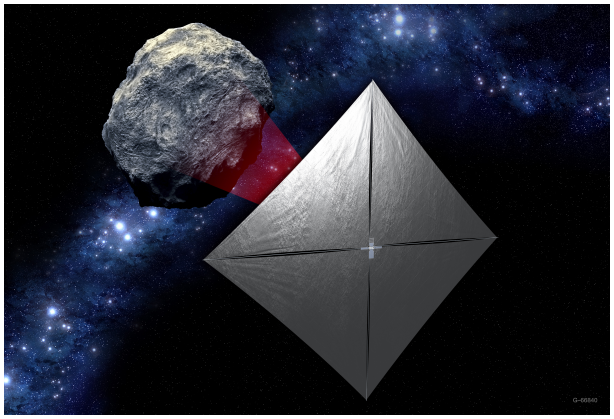

(**d**)

Figure 18. Illustration of various mitigation technologies of: (**a**) gravity tractor [155]; (**b**) focused solar energy [156]; (**c**) the deployment scheme of DART mission [157]; and (**d**) the conceptual design of solar sail [158].

Table 2. A summary of representative mitigation technologies.

Energy Source	Approach	Strategy	Key Technology and Features	Example	Comments
Nuclear Explosive Device	Stand-off approach	Interception and trajectory-changing	Denotation at 20-m or greater stand-off height; 10–100 times more effective than the non-nuclear alternatives	Project Icarus MIT Students [88]; NASA's asteroid Interceptor "Cradle spacecraft" in [159]	In [88], a number of modified Satrun V rockets and creation of nuclear explosive devices in the 100-megaton energy range; In [159], the conceptual spacecraft contains six B83 physics packages with each set for 1.2-megaton yield and and to be detonated over a 100-m height.
	Surface and subsurface	Interception and trajectory-changing	Creation of a conceptual Hypervelocity Asteroid Intercept Vehicle (HAIV), which combines a kinetic impactor to create an initial crater for a follow-up subsurface nuclear detonation within that initial crater	HAIV can cope with 50–500-m diameter objects when the time to Earth impact is less than one year [160]; With a warning time of 30 days, a 300-m wide asteroid can be neutralized by a single HAIV with less than 0.1% of the PHO's mass [161]	HAIV can generate high degree of efficiency in the conversion of the nuclear energy that is released in the detonation into propulsion energy to the asteroid; It may run an increased risk of fracturing the target NEO.
	Comet Deflection	Interception and vaporize or trajectory-changing	One-gigaton nuclear explosive device weighting 25–30 tons, lifted on super-heavy rocket	Dr. Edward Teller proposed in 1995 Planetary Defense workshop [162]	Instantly vaporize a 1-km asteroid or divert a 10-km one; It can cope with short-period comets escaping from the Kuiper belt.
Kinetic Impact	Kinetic impactor deflection	Interception and trajectory-changing	Sending spacecraft to a collision course to knock off the asteroid	NEOShield-2 mission from ESA [163]; Asteroid Impact and Deflection Assessment (AIDA) missions of ESA/NASA, DART launched in November 2021 [7,164]	The DART impact will occur in October 2022 and allow Earth-based telescopes and planetary radar to observe the event.
Asteroid Gravity Tractor	Apply a small but constant thrust	Rendezvous with PHO and provide a small force	A massive unmanned spacecraft hovering over an asteroid to gravitationally pull the asteroid into a non-threatening orbit	Edward T. Lu and Stanley G. Love proposed [165]	The most expensive with the lowest technical readiness and many years to decades of duration might be required.
Focused Solar Energy	Focus solar energy onto PHO's surface	Remote station and rendezvous	Construction of remote station with large concave mirrors, concentration is scalable	Proposed in [166]; Ring-array collector size is 0.5 PHO's diameter [167]	In [167], 5000 times the sunlight concentration, 1000-N thrusting effect, forming gas flow.
Asteroid Laser Ablation	Focus laser onto PHO's surface	Rendezvous and trajectory -changing	Concentrate laser energy to cause flash vaporization/ablation with reaction force	First proposed in [168]; Project DE-STAR, proposed [169]	Ref. [169] phased-array laser about 1 km squared, launched in increments assembled in space.
Ion Beam Shepherd	Pointing ion thruster at PHO's surface	Interception and trajectory -changing	Use the momentum transmitted by a low-divergence (<15 deg) accelerated ion beam	First proposed in [170]	A 5-ton space debris can be deorbited in about 7 months with IBS mass less than 300 kg.

In addition, some other proposed deflection methods include wrapping the PHO in a sheet of reflective plastic such as aluminized polyethylene terephthalate (PET) as a solar sail; dusting the PHO with titanium dioxide (white) to alter its trajectory via increasing the reflected radiation pressure or with black to alter its trajectory via the Yarkovsky effect;

attaching a mass driver on the PHO to eject material into space to give the PHO a slow steady push and decrease its mass; deploying coherent digging/mining array multiple 1-ton flat tractors able to dig and expel PHO's soil mass as a coherent fountain array [171]; attaching a tether and ballast mass to the PHO to alter its mass center and trajectory; and using magnetic flux compression to magnetically brake and or capture a PHO that contains a high percentage of meteoric iron by deploying a wide coil of wire in its orbital path [172].

The multi-layered architecture of the SCADN network can detect and mitigate the PHO more effectively. On top of a deep understanding of the characteristics of mainstream PHO mitigation technologies, the SCADN framework is equipped with various types of mitigation strategies with several key points unfolded as follows:

1. Ideally, a hybrid of PHO deflection schemes can be deployed to the spacecraft in each planet's Lagrange points. For example, in remote areas such as around Saturn, Uranus, or Neptune, the low-cost and slow-paced schemes (non-nuclear scheme) can work over an allowable time window that is usually large enough. For example, whenever a space object is detected and determined to be a threat to Earth or other humans' colonization by the SCADN, one or more spacecraft patrolling in the nearest proximity or being able to intercept the PHO on its collision course will be scheduled and coordinated to handle the mitigation.
2. If the situation is so urgent that a fast response is needed immediately, the decision making, resource allocation, task scheduling, and trajectory planning can be fully autonomous, e.g., completely directed by AI/edge-computing, to overcome the large latency in space communication (due to the extremely large space travel distance). The early detection and mitigation will result in lower cost and a higher success rate of mitigation. The power supply can be a hybrid source of nuclear battery and solar panel, while the propulsive devices can be of various types, e.g., cold gas thruster, electrohydrodynamic thruster, electrodeless plasma thruster, electrostatic ion thruster, Hall effect thruster, magnetoplasmadynamic thruster, etc.
3. An illustrative description of an exemplary application scenario is presented in Figure 19a, where a space object is detected and identified as having a high probability of impacting Earth within less than one year. The SCADN framework calculates its trajectory (in the red dash line), determines its mass and characteristics, and makes feasible mitigation strategies and plans. Eventually, the SCADN schedules the available spacecraft equipped with suitable mitigation technologies to intercept the object. During this procedure, the spacecraft perhaps need to change its orbit, accelerate or decelerate, which can lead to the consumption of power and thrust on board the spacecraft. In case one spacecraft fails a mitigation task, SCADN can call for multiple spacecraft simultaneously from different orbital locations of different planets to perform the interception.
4. The SCADN framework is capable of computing and mobilizing all available resources within its framework to monitor any space object sensed, estimate the risk, and take the corresponding actions. Such a SCADN framework is supposed to be robust enough that it can still be functional to detect and mitigate the risk even when some spacecraft/survey stations within the framework cannot work properly or human operators are not available. A brief flow chart of the SCADN is given in Figure 19b, where the SCADN framework will utilize all available spacecraft to perform the interception until the impact risk is completely neutralized. Since all spacecraft being able to conduct the mitigation missions are continuously on alert in space, the success rate is largely improved compared to any improvisational interception launch mission from Earth.

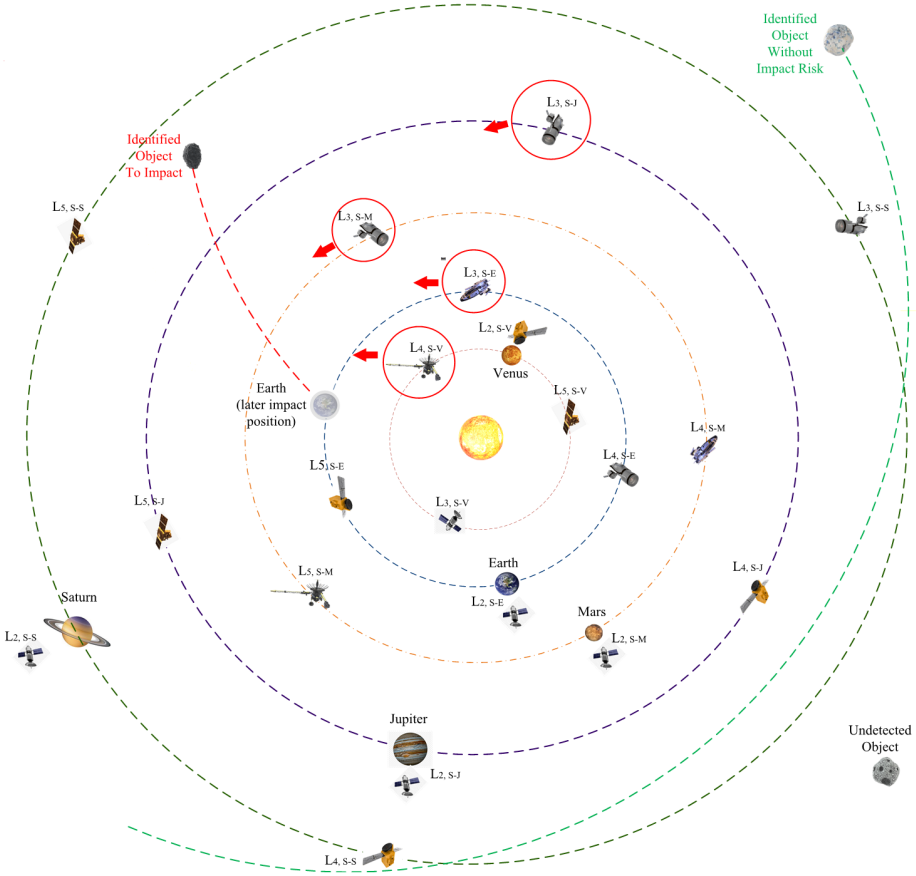

(**a**)

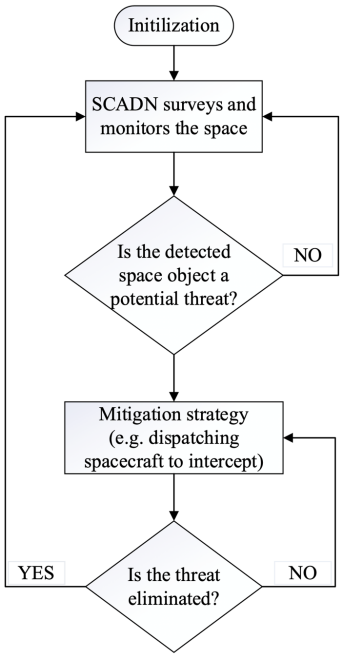

(**b**)

Figure 19. (**a**) Illustration of the SCADN framework which monitors the space and detects and intercepts the hazardous space objects (dimension of celestial bodies, space objects, and orbits are not scaled); and (**b**) a brief flowchart of the SCADN framework.

Moreover, some simulations and numerical analyses are conducted and presented in light of the channel physical characteristics of deep space wireless communications within the SCADN framework. The substantial path losses and latency vary as the positions among celestial bodies change significantly over time. Some parameters of interest, such as distance, free-space path loss (FSPL), and latency, are given and compared in Figure 20 for several exemplary cases. The distances are in the unit of AU and categorized into relatively large and small values (but not the maximum and minimum values).

Object/ Parameters	Distance to Earth (Large) (AU)	Free-Space Path Loss (Large) (dB)		Latency (Large) (s)	Distance to Earth (Small) (AU)	Free-Space Path Loss (Small) (dB)		Latency (Large) (s)
		2.3 GHz	8.4 GHz			2.3 GHz	8.4 GHz	
Venus	1.7170	267.8761	279.1272	856.8	0.2886	252.3874	263.6384	144.0
Mars	2.5233	271.2201	282.4711	1259.1	0.5444	257.8994	269.1505	271.7
Jupiter	5.9540	278.677	289.928	2971.1	3.9563	275.1265	286.3776	1974.2
Saturn	10.8109	283.8581	295.1091	5394.7	8.8564	282.1260	293.3770	4419.4
Voyager 1	155.6813*	307.0256	318.2766	77685.7	N.A.			

* As of May 25, 2022.

(**a**)

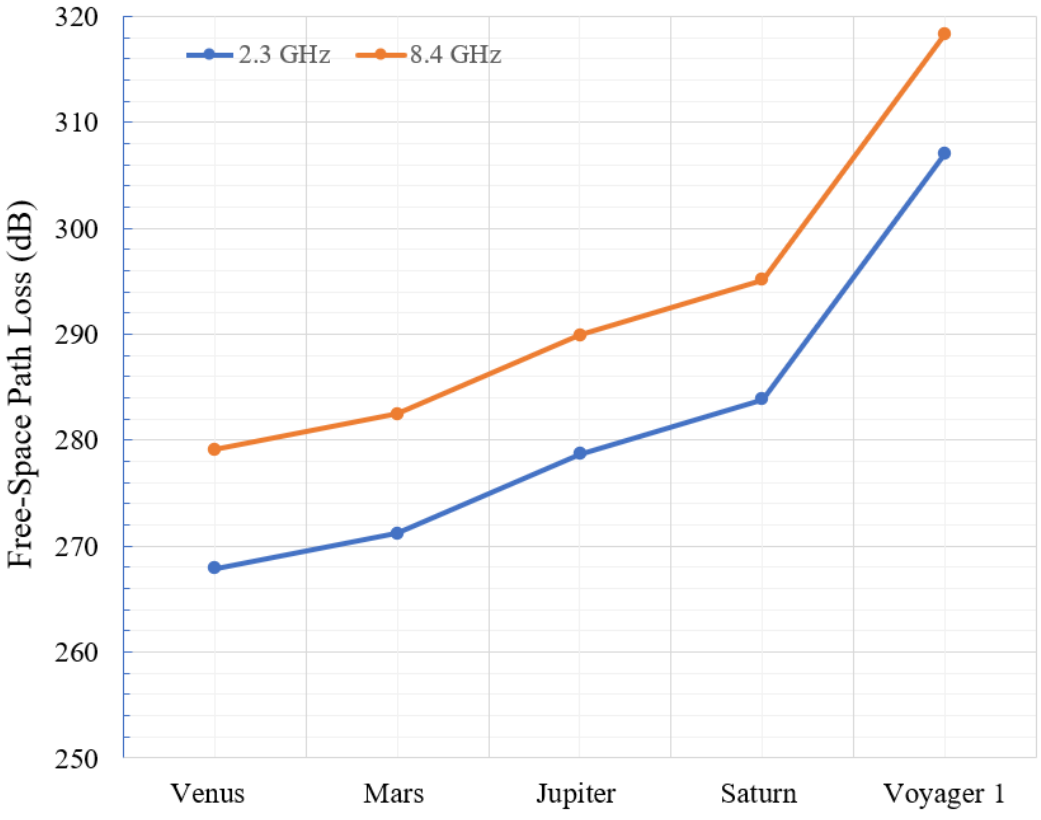

(**b**)

Figure 20. (**a**) Comparison of parameters of interest for Venus, Mars, Jupiter, Saturn, and Voyager 1; and (**b**) Comparison of free-space path loss (large distances for planets) at 2.3 GHz and 8.4 GHz, respectively.

Last but not least, understanding the celestial bodies' movement and orbits and the channel characteristics on top of them will essentially help design the communication

systems onboard the spacecraft/spaceships, plus the trajectory and orbital plans. This part of investigation can be put into a more detailed future study.

5.3. Long-Term Universal Efforts

Planning, developing, deploying, maintaining, and upgrading such a huge SCADN framework would require significant resources and efforts across many various entities. There will be expectations of critical collaborations among space agencies (e.g., NASA, ESA), governments, intergovernmental organizations (e.g., EU, ITU), research facilities, technical and professional associations (e.g., IEEE, AIAA), and technological corporations (e.g., SpaceX, Blue Origin), etc.

Furthermore, the legislation of related laws and standards is another critical success factor. The famous astronomer and planetary scientist Dr. Carl Sagan expressed concern about deflection technology in his book *Pale Blue Dot* [173] where he noted that any method capable of deflecting space objects away from Earth could also be abused to divert non-threatening bodies toward the planet. Therefore, rigorous legislation and implementation are of the highest priority and importance during the top-down design of the proof-of-concept (PoC). For example, efficient public supervision and timely disclosure may help improve the eventual success of the SCADN framework. Also, developing and widely adopting advanced AI algorithms can decrease the unauthorized manipulation or mistakes of manual operations and enhance the cyber-security and overall performance of the SCADN framework. The authorization of upgrading the framework and core AI algorithms may require the highest-level granting from multiple entities to best serve the common interest of all humankind.

In addition, several related international treaties should be taken into account when planning and developing the SCADN framework. The first is the Treaty on the Non-Proliferation of Nuclear Weapons, commonly known as the Non-Proliferation Treaty (NPT). It aims at preventing the spread of nuclear weapons and weapons technology to promote cooperation in using nuclear energy peacefully, with a further target of achieving nuclear disarmament, including general and complete disarmament [174]. The second one is The Outer Space Treaty (OST), formally the Treaty on Principles Governing the Activities of States in the Exploration and Use of Outer Space, including the Moon and other celestial bodies. The OST is a multilateral treaty that forms the basis of international space law. In particular, it has included several key provisions such as prohibiting nuclear weapons in space and limiting the use of the Moon and all other celestial bodies to peaceful purposes [175]. Consequently, there is a necessity for considerable investigation of the asteroid/comet mitigation technologies under both NPT and OST. The SCADN framework is likely to comply with these treaties since early detection can enable the use of slow and steady mitigation technologies.

Moreover, fully deploying the SCADN framework may take significant time. Dividing the construction into several stages is thus reasonable and also feasible. For example, Phase I of the SCADN framework can target the coverage of the area reaching Jupiter. It is also noteworthy that several factors need to be considered as they can interrupt the progress to some extent. For instance, the global supply chain can be disrupted during emergencies such as wars and pandemics [176].

6. Conclusions

In this paper, a comprehensive review of space exploration, space colonization, space threats, extinction events, space observatory, and space defense has been given, followed by a detailed presentation of related research and projects on milestones in human history. Furthermore, a summary and a prediction are made for humanity's future evolution path: terraforming other celestial bodies for extra-terrestrialization. As a result, multi-planet-based communications and defense networks will be critically necessary, and a framework named the Solar Communication and Defense Networks (SCADN) is proposed and analyzed. The distributed and intelligent features of the proposed SCADN framework

can provide high reliability in coping with the potentially hazardous space objects in emergent situations and serve other purposes of space exploration and astronomical survey. Eventually, it is envisioned that founding such an enormous framework may require unprecedented resources and efforts across many nations and entities on a long-term basis for human living and prosperity. To utilize such a framework to serve the entire human race's common interest under international treaties, strict legislation, scientific implementation, and public supervision will play a crucial role.

7. Future Research Directions

Several aspects of future research can be carried on:

1. The trajectory and orbital plans need to be designed and verified to estimate the technological feasibility, expense of resources, the time of development, and deployment.
2. The PHOs mitigation technologies need to be well investigated and developed, particularly for the feasible clean type compatible with international treaties.
3. The AI and edge-computing-aided wireless communications and networking technologies for deep-space sensing and communications need to be thoroughly investigated.

There are more diverse research directions for researchers from various backgrounds to accelerate the unprecedented transformation of humanity's future life.

Funding: This research received no external funding.

Institutional Review Board Statement: Not applicable.

Informed Consent Statement: Not applicable.

Data Availability Statement: Not applicable.

Acknowledgments: The author would like to express sincere gratitude to the great minds and pioneers who have dedicated their efforts and even life to astronomy and space exploration.

Conflicts of Interest: The author declares no conflict of interest.

References

1. Armstrong, N. Buzz Aldrin Removing the Passive Seismometer from a Compartment in the SEQ Bay of the Lunar Lander. 21 July 1969. Available online: https://en.wikipedia.org/wiki/File:Apollo_11_Lunar_Lander_-_5927_NASA.jpg (accessed on 8 May 2022).
2. NASA. The SpaceX Crew Dragon Spacecraft, with Its Nose Cone Open, is Pictured Docked to the Harmony Module's forward International Docking Adapter. Available online: https://images.nasa.gov/details-iss064e027440 (accessed on 8 May 2022).
3. NASA/Crew-2. The International Space Station is Pictured from the SpaceX Crew Dragon Endeavour during a Flyaround of the Orbiting Lab that Took Place Following Its Undocking from the Harmony Module's Space-Facing Port on 8 November 2021. 8 November 2021. Available online: https://commons.wikimedia.org/wiki/File:View_of_the_ISS_taken_during_Crew-2_flyaround_(ISS066-E-081311).jpg (accessed on 8 May 2022).
4. NASA. The Hubble Space Telescope (HST) Begins Its Separation from Space Shuttle Discovery Following Its Release on Mission STS-82. 1997. Available online: https://apod.nasa.gov/apod/ap021124.html (accessed on 8 May 2022).
5. NASA/JPL. PIA03883: Artists's Conception of Cassini Saturn Orbit Insertion. 2002. Available online: https://photojournal.jpl.nasa.gov/catalog/PIA03883 (accessed on 8 May 2022).
6. European Space Agency. Rosetta and Philae at Comet: Artist's Impression of the Rosetta Orbiter Deploying the Philae Lander to Comet 67P/Churyumov–Gerasimenko. 2013. Available online: https://www.flickr.com/photos/europeanspaceagency/11206660686/ (accessed on 8 May 2022).
7. Adams, E.; O'Shaughnessy, D.; Reinhart, M.; John, J.; Congdon, E.; Gallagher, D.; Abel, E.; Atchison, J.; Fletcher, Z.; Chen, M.; et al. Double Asteroid Redirection Test: The Earth Strikes Back. In Proceedings of the IEEE Aerospace Conference, Big Sky, MT, USA, 2–9 March 2019; pp. 1–11. [CrossRef]
8. Ackerman, E. SpaceX Planning to Land Autonomous Reusable Rockets on Drone Ships. Available online: https://spectrum.ieee.org/spacex-planning-to-land-autonomous-reusable-rockets-on-drone-ships-next-month (accessed on 8 May 2022).
9. Krahn, J. Starship SN9 Sitting on Its Launch Pad in Starbase. Available online: https://commons.wikimedia.org/wiki/File:Starship_SN9_Launch_Pad.jpg (accessed on 8 May 2022).
10. Seife, C. Dark energy tiptoes toward the spotlight. *Science* **2003**, *300*, 1896–1897. [CrossRef] [PubMed]
11. Brumfiel, G. How they wonder what you are. *Nature* **2008**. [CrossRef]

12. Reichhardt, T. Is the next big thing too big? *Nature* **2006**, *440*, 140–143. [CrossRef]
13. Billings, L. Space science: The telescope that ate astronomy. *Nature* **2010**, *467*, 1028–1030. [CrossRef] [PubMed]
14. NASA/Goddard Space Flight Center/Pat Izzo. The Full-Scale Model is Assembled on the Lawn at Goddard Space Flight Center, and Displayed during 19–25 September 2005. 2005. Available online: https://www.jwst.nasa.gov/images/people.jpg (accessed on 8 May 2022).
15. Hansen, C.J.; Esposito, L.; Stewart, A.I.F.; Colwell, J.; Hendrix, A.; Pryor, W.; Shemansky, D.; West, R. Enceladus' water vapor plume. *Science* **2008**, *311*, 1422–1425. [CrossRef] [PubMed]
16. Hansen, C.J.; Esposito, L.W.; Stewart, A.I.F.; Meinke, B.; Wallis, B.; Colwell, J.E.; Hendrix, A.R.; Larsen, K.; Pryor, W.; Tian, F. Water vapour jets inside the plume of gas leaving Enceladus. *Nature* **2008**, *456*, 477–479. [CrossRef] [PubMed]
17. Bertotti, B.; Iess, L.; Tortora, P. A test of general relativity using radio links with the Cassini spacecraft. *Nature* **2003**, *425*, 374–376. [CrossRef] [PubMed]
18. Butler, D. Spiralling costs dog comet mission. *Nature* **2003**, *423*, 372–373. [CrossRef]
19. Gibney, E. Historic Rosetta mission to end with crash into comet. *Nature* **2015**, *527*, 16–17. [CrossRef]
20. Gibney, E. Mission accomplished: Rosetta crashes into comet. *Nature* **2016**, *538*, 13–14. [CrossRef]
21. Vernazza, P.; Ferrais, M.; Jorda, L.; Hanuš, J.; Carry, B.; Marsset, M.; Brož, M.; Fetick, R.; Viikinkoski, M.; Marchis, F.; et al. VLT/SPHERE imaging survey of the largest main-belt asteroids: Final results and synthesis. *Astron. Astrophys.* **2021**, *654*, A56. [CrossRef]
22. Elkins-Tanton, L.T.; Asphaug, E.; Bell, J.; Bercovici, D.; Bills, B.G.; Binzel, R.P.; Bottke, W.F.; Jun, I.; Marchi, S.; Oh, D.; et al. Journey to a metal world: Concept for a Discovery Mission to Psyche. In Proceedings of the 45th Lunar and Planetary Science Conference, The Woodlands, TX, USA, 17–21 March 2014.
23. Shear, W. The early development of terrestrial ecosystems. *Nature* **1991**, *351*, 283–289. [CrossRef]
24. Garwood, R.J.; Edgecombe, G.D. Early terrestrial animals, evolution, and uncertainty. *Evol. Educ. Outreach* **2011**, *4*, 489–501. [CrossRef]
25. MacIver, M.; Schmitz, L.; Mugan, U.; Murphey, T.; Mobley, C. Massive increase in visual range preceded the origin of terrestrial vertebrates. *Proc. Natl. Acad. Sci. USA* **2017**, *114*, E2375–E2384. 10.1073/pnas.1615563114. [CrossRef]
26. Musk, E. Making humans a multi-planetary species. *New Space* **2017**, *5*, 46–61. [CrossRef]
27. Musk, E. Making life multi-planetary. *New Space* **2018**, *6*, 2–11. [CrossRef]
28. Musk, E. Risky Business. *IEEE Spectr.* **2009**, *46*, 40–41. [CrossRef]
29. Jones, H.W. The recent large reduction in space launch cost. In Proceedings of the 48th International Conference on Environmental Systems, New Mexico, FL, USA, 8–12 July 2018.
30. Koelle, D.E. *TRANSCOST, Statistical-Analytical Model for Cost Estimation and Economic Optimization of Space. Transportation Systems*; MBB Report; URV-185; Raumtransportsysteme und Antriebe, Deutsche Aerospace: Köln, Germany, 1991.
31. NASA. Advanced Space Transportation Program: Paving the Highway to Space. Available online: https://www.nasa.gov/centers/marshall/news/6 (accessed on 8 May 2022).
32. SpaceX. Starship Users Guide. Revision1. 2020. Available online: https://www.spacex.com/starship/7 (accessed on 8 May 2022).
33. Mann, A. SpaceX Now Dominates Rocket Flight, Bringing Big Benefits and Risks to NASA. Available online: https://www.science.org/content/article/spacex-now-dominates-rocket-flight-bringing-big-benefits-and-risks-nasa (accessed on 20 May 2022).
34. Georgina, T. SpaceX's Hexagon Heat Shield Tiles Take on an Industrial Flamethrower. Digital Trends. 2019. Available online: https://www.digitaltrends.com/cool-tech/spacex-hexagon-heat-shield-tiles/ (accessed on 8 May 2022).
35. McKay, C.; Toon, O.; Kasting, J. Making Mars habitable. *Nature* **1991**, *352*, 489–496. [CrossRef]
36. Kasting, J. Warming early Earth and Mars. *Science* **1997**, *276*, 1213. [CrossRef]
37. Tosca, N.J.; Knoll, A.H.; McLennan, S.M. Water activity and the challenge for life on early Mars. *Science* **2008**, *320*, 1204–1207. [CrossRef]
38. McEwen, A.S.; Ojha, L.; Dundas, C.M.; Mattson, S.S.; Byrne, S.; Wray, J.J.; Cull, S.C.; Murchie, S.L.; Thomas, N.; Gulick, V.C. Seasonal flows on warm Martian slopes. *Science* **2011**, *333*, 740–743. [CrossRef] [PubMed]
39. JPL. Seasonal Changes in Mars' North Polar Ice Cap. 1998. Available online: https://www.jpl.nasa.gov/images/pia01247-seasonal-changes-in-mars-north-polar-ice-cap (accessed on 8 May 2022).
40. Sanders, G. Mars ISRU: State-of-the-Art and System Level Considerations. 2016. Available online: Http://kiss.caltech.edu/workshops/isru/presentations/Sanders.pdf (accessed on 8 May 2022).
41. Rönsch, S.; Schneider, J.; Matthischke, S.; Schlüter, M.; Götz, M.; Lefebvre, J.; Prabhakaran, P.; Bajohr, S. Review on methanation—From fundamentals to current projects. *Fuel* **2015**, *166*, 276–296. [CrossRef]
42. Gibney, E. How to build a Moon base. *Nature* **2018**, *562*, 474–478. [CrossRef] [PubMed]
43. Hepp, A.F.; Linne, D.L.; Landis, G.A.; Wadel, M.F.; Colvin, J.E. Production and use of metals and oxygen for lunar propulsion. *J. Propuls. Power* **1994**, *10*, 834–840. [CrossRef]
44. Wittenberg, L.J.; Cameron, E.N.; Kulcinski, G.L.; Ott, S.H.; Santarius, J.F.; Sviatoslavsky, G.I.; Sviatoslavsky, I.N.; Thompson, H.E. A Review of ^{3}He Resources and Acquisition for Use as Fusion Fuel. *Fusion Technol.* **1992**, *21*, 2230–2253. [CrossRef]
45. NASA. Moon to Mars Overview. Available online: https://www.nasa.gov/topics/moon-to-mars/overview (accessed on 8 May 2022).

46. Dorminey, B. Why the Moon should Never be Terraformed. Forbes. 2016. Available online: https://www.forbes.com/sites/brucedorminey/2016/07/27/why-the-moon-should-never-be-terraformed/?sh=8f089914ed98 (accessed on 8 May 2022).
47. Benford, G. How to Terraform the Moon. Slate. 2014. Available online: https://slate.com/technology/2014/07/terraforming-the-moon-it-would-be-a-lot-like-florida.html (accessed on 8 May 2022).
48. Kargel, J. *Mars: A Warmer, Wetter Planet*; Springer: Berlin/Heidelberg, Germany, 2004; ISBN 1-85233-568-8.
49. Schubert, G.; Turcotte, D.; Olson, P. *Mantle Convection in the Earth and Planets*; Cambridge University Press: Cambridge, UK, 2001; ISBN 0-521-79836-1.
50. Forget, F.; Lognonné, P.; Costard, F. *Planet Mars: Story of Another World*; Springer: Berlin/Heidelberg, Germany, 2007; ISBN 0-387-48925-8.
51. Philips, T. Solar Wind Rips up Martian Atmosphere. 2008. Available online: https://science.nasa.gov/science-news/science-at-nasa/2008/21nov_plasmoids (accessed on 8 May 2022).
52. Wall, M. Elon Musk Floats 'Nuke Mars' Idea Again (He Has T-Shirts). 2019. Available online: https://www.space.com/elon-musk-nuke-mars-terraforming.html (accessed on 8 May 2022).
53. Faure, G.; Mensing, M. *Introduction to Planetary Science: The Geological Perspective*; Springer: Berlin/Heidelberg, Germany, 2007; ISBN 1-4020-5233-2.
54. Forget, F.; Pierrehumbert, R.T. Warming early Mars with carbon dioxide clouds that scatter infrared radiation. *Science* **1997**, *278*, 1273–1276. [CrossRef]
55. Wordsworth, R.; Kerber, L.; Cockell, C. Enabling Martian habitability with silica aerogel via the solid-state greenhouse effect. *Nat. Astron.* **2019**, *3*, 898–903. [CrossRef]
56. Lopez, J. Inevitable future: Space colonization beyond Earth with microbes first. *FEMS Microbiol. Ecol.* **2019**, *95*, fiz127. [CrossRef]
57. Renne, P.R.; Deino, A.L.; Hilgen, F.J.; Kuiper, K.F.; Mark, D.F.; Mitchell, W.S., III; Morgan, L.E.; Mundil, R.; Smit, J. Time scales of critical events around the Cretaceous-Paleogene boundary. *Science* **2013**, *339*, 684–687. [CrossRef]
58. Nichols, D.; Johnson, K. *Plants and the K–T Boundary*; Cambridge University Press: Cambridge, UK, 2008.
59. Longrich, N.R.; Tokaryk, T.; Field, D.J. Mass extinction of birds at the Cretaceous–Paleogene (K–Pg) boundary. *Proc. Natl. Acad. Sci. USA* **2011**, *108*, 15253–15257. [CrossRef]
60. Longrich, N.R.; Bhullar, B.A.S.; Gauthier, J.A. Mass extinction of lizards and snakes at the Cretaceous–Paleogene boundary. *Proc. Natl. Acad. Sci. USA* **2012**, *109*, 21396–21401. [CrossRef]
61. Friedman, M. Ecomorphological selectivity among marine teleost fishes during the end-Cretaceous extinction. *Proc. Natl. Acad. Sci. USA* **2009**, *106*, 5218–5223. [CrossRef]
62. Hildebr, A.R.; Penfield, G.T.; Kring, D.A.; Pilkington, M.; Camargo, Z.A.; Jacobsen, S.B.; Boynton, W.V. Chicxulub crater: A possible Cretaceous/Tertiary boundary impact crater on the Yucatán peninsula, Mexico. *Geology* **2009**, *19*, 867–871. [CrossRef]
63. Schulte, P. The Chicxulub asteroid impact and Mass Extinction at the Cretaceous-Paleogene boundary. *Science* **2010**, *327*, 1214–1218. [CrossRef]
64. Durand-Manterola, H.; Cordero-Tercero, G. Assessments of the Energy, Mass and Size of the Chicxulub Impactor. *arXiv* **2014**, arXiv:1403.6391.
65. Robertson, D.S.; Lewis, W.M.; Sheehan, P.M.; Toon, O.B. K/Pg extinction: Re-evaluation of the heat/fire hypothesis. *J. Geophys. Res. Biogeosc.* **2013**, *118*, 329–336. [CrossRef]
66. Chiarenza, A.A.; Farnsworth, A.; Mannion, P.D.; Lunt, D.J.; Valdes, P.J.; Morgan, J.V.; Allison, P.A. Asteroid impact, not volcanism, caused the end-Cretaceous dinosaur extinction. *Proc. Natl. Acad. Sci. USA* **2020**, *117*, 17084–17093. [CrossRef]
67. Alroy, J. The fossil record of North American Mammals: Evidence for a Palaeocene evolutionary radiation. *Syst. Biol.* **1998**, *48*, 107–118. [CrossRef]
68. Rasmussen, S.O.; Andersen, K.K.; Svensson, A.M.; Steffensen, J.P.; Vinther, B.M.; Clausen, H.B.; Siggaard-Andersen, M.-L.; Johnsen, S.J.; Larsen, L.B.; Dahl-Jensen, D.; et al. A new Greenland ice core chronology for the last glacial termination. *J. Geophys. Res.* **2006**, *111*. [CrossRef]
69. Firestone, R.B.; West, A.; Kennett, J.P.; Becker, L.; Bunch, T.E.; Revay, Z.S.; Schultz, P.H.; Belgya, T.; Kennett, D.J.; Erlandson, J.M.; et al. Evidence for an extraterrestrial impact 12,900 years ago that contributed to the megafaunal extinctions and the Younger Dryas cooling. *Proc. Natl. Acad. Sci. USA* **2007**, *2104*, 16016–16021. [CrossRef]
70. Bunch, T.E.; Hermes, R.E.; Moore, A.M.; Kennett, D.J.; Weaver, J.C.; Wittke, J.H.; DeCarli, P.S.; Bischoff, J.L.; Hillman, G.C.; Howard, G.A.; et al. Very high-temperature impact melt products as evidence for cosmic airbursts and impacts 12,900 years ago. *Proc. Natl. Acad. Sci. USA* **2012**, *109*, 1903–1912. [CrossRef]
71. Kennett, D.J.; Kennett, J.P.; West, A.; Mercer, C.; Hee, S.S.Q.; Bement, L.; Bunch, T.E.; Sellers, M.; Wolbach, W.S. Nanodiamonds in the Younger Dryas boundary sediment layer. *Science* **2009**, *323*, 94. [CrossRef] [PubMed]
72. Kinzie, C.R.; Hee, S.S.Q.; Stich, A.; Tague, K.A.; Mercer, C.; Razink, J.J.; Kennett, D.J.; DeCarli, P.S.; Bunch, T.E.; Wittke, J.H.; et al. Nanodiamond-rich layer across three continents consistent with major cosmic impact at 12,800 cal BP. *J. Geol.* **2014**, *122*, 475–506. [CrossRef]
73. Jenniskens, P. Tunguska eyewitness accounts, injuries and casualties. *Icarus* **2019**, *327*, 4–18. [CrossRef]
74. Farinella, P.; Foschini, L.; Froeschlé, C.; Gonczi, R.; Jopek, T.; Longo, G.; Michel, P. Probable asteroidal origin of the Tunguska cosmic body. *Astron. Astrophys.* **2001**, *377*, 1081–1097. [CrossRef]
75. De Pater, I.; Lissauer, J. *Planetary Sciences*; Cambridge University Press: Cambridge, UK, 2001; ISBN 0521482194.

76. Nemiroff, R. Unguska: The Largest Recent Impact Event. NASA. 2007. Available online: https://apod.nasa.gov/apod/ap071114.html (accessed on 8 May 2022).
77. Whipple, F. On Phenomena related to the great Siberian meteor. *Q. J. R. Meteorol. Soc.* **1934**, *257*, 505–522. [CrossRef]
78. Watson, N. The Tunguska Event. *Hist. Today* **2008**, *58*. Available online: https://www.historytoday.com/archive/tunguska-event (accessed on 8 May 2022).
79. Turco, R.; Toon, O.; Park, C.; Whitten, R.; Pollack, J.; Noerdlinger, P. An analysis of the physical, chemical, optical and historical impacts of the 1908 Tunguska meteor fall. *Icarus* **1982**, *50*, 1–52. [CrossRef]
80. Popova, O.P.; Jenniskens, P.; Emel'Yanenko, V.; Kartashova, A.; Biryukov, E.; Khaibrakhmanov, S.; Shuvalov, V.; Rybnov, Y.; Dudorov, A.; Grokhovsky, V.I.; et al. Chelyabinsk airburst, damage assessment, meteorite recovery, and characterization. *Sicence* **2013**, *342*, 1069–1073. [CrossRef] [PubMed]
81. Schiermeier, Q. Risk of massive asteroid strike underestimated. *Nature* **2013**. [CrossRef]
82. Brown, P. A 500-kiloton airburst over Chelyabinsk and an enhanced hazard from small impactors. *Nature* **2013**, *503*, 238–241. [CrossRef]
83. Yeomans, D.; Chodas, P. Additional Details on the Large Fireball Event over Russia on 15 February 2013. NASA/JPL Near-Earth Object Program Office. 2013. Available online: https://cneos.jpl.nasa.gov/news/fireball_130301.html (accessed on 8 May 2022).
84. Brown, P.H.; Spalding, R.E.; O Revelle, D.; Tagliaferri, E.; Worden, S.P. The flux of small near-Earth objects colliding with the Earth. *Nature* **2002**, *420*, 294–296. [CrossRef] [PubMed]
85. Borovička, J.; Spurný, P.; Brown, P.G.; A Wiegert, P.; Kalenda, P.; Clark, D.; Shrbený, L. The trajectory, structure and origin of the Chelyabinsk asteroidal impactor. *Nature* **2013**, *503*, 235–237. [CrossRef]
86. Melosh, H.; Collins, G. Meteor Crater formed by low-velocity impact. *Nature* **2005**, *434*, 157. [CrossRef] [PubMed]
87. Cole, D.; Cox, D. *Islands in Space: The Challenge of the Planetoids*; Chilton Books: Sudbury, UK, 1964.
88. Day, D. Giant Bombs on Giant Rockets: Project Icarus. The Space Review, 5 July 2004. Available online: https://www.thespacereview.com/article/175/1 (accessed on 8 May 2022).
89. Alvarez, L.W.; Alvarez, W.; Asaro, F.; Michel, H.V. Extraterrestrial cause for the Cretaceous-Tertiary extinction: Experiment and theory. *Science* **1980**, *208*, 1095–1108. [CrossRef] [PubMed]
90. Canavan, G. *Proceedings of the Near-Earth-Object Interception Workshop*; Los Alamos National Laboratory: Los Alamos, NM, USA, 1992.
91. Morrison, D. The Spaceguard Survey: Report of the NASA International Near-Earth-Object Detection Workshop. 1992. Available online: https://archive.org/details/nasa_techdoc_19920025001 (accessed on 8 May 2022).
92. Harris, A. What spaceguard did. *Nature* **2008**, *453*, 1178–1179. [CrossRef] [PubMed]
93. Yeomans, D. Testimony before the House Committee on Science and Technology Subcommittee on Space and Aeronautics: Near-Earth Objects (NEOS)—Status of the Survey Program and Review of Nasa's Report to Congress. 2007. Available online: https://web.archive.org/web/20080131081137/http://democrats.science.house.gov/media/File/Commdocs/hearings/2007/space/08nov/Yeomans_testimony.pdf (accessed on 8 May 2022).
94. Martin, P. NASA's Efforts to Identify Near-Earth Objects and Mitigate Hazards. NASA Office of Inspector General. 2014. Available online: https://oig.nasa.gov/audits/reports/FY14/IG-14-030.pdf (accessed on 8 May 2022).
95. NASA. Planetary Defense Frequently Asked Questions. Available online: https://www.nasa.gov/planetarydefense/faq (accessed on 8 May 2022).
96. Lunar and Planetary Science. Catalina Sky Survey. Available online: https://catalina.lpl.arizona.edu/ (accessed on 8 May 2022).
97. Lunar and Planetary Science. Catalina Sky Survey Discovers Space Rock That Could Hit Mars. Available online: https://news.arizona.edu/story/catalina-sky-survey-discovers-space-rock-could-hit-mars (accessed on 8 May 2022).
98. Broad, W. Agencies, Hoping to Deflect Comets and Asteroids, Step Up Earth Defense. The New York Times. 2015. Available online: https://www.nytimes.com/2015/06/19/science/agencies-make-plans-to-step-up-planetary-defense.html (accessed on 8 May 2022).
99. NASA. Planetary Defense Coordination Office. Available online: https://www.nasa.gov/planetarydefense/overview (accessed on 8 May 2022).
100. Brown, D.; Neal-Jones, N. NASA's OSIRIS-REx Mission Passes Critical Milestone. NASA. Release 15-056. 2015. Available online: https://www.nasa.gov/press/2015/march/nasa-s-osiris-rex-mission-passes-critical-milestone (accessed on 8 May 2022).
101. NASA. OSIRIS-REx Mission Selected for Concept Development. Available online: https://web.archive.org/web/20120606151314/http://gsfctechnology.gsfc.nasa.gov/ORIRIS.htm (accessed on 8 May 2022).
102. Wall, M. NASA's OSIRIS-REx Probe Successfully Stows Space-Rock Sample. Scientific American. 2020. Available online: https://www.scientificamerican.com/article/nasas-osiris-rex-probe-successfully-stows-space-rock-sample/ (accessed on 8 May 2022).
103. WISE Public Web Site. Wide-Field Infrared Survey Explorer. Available online: https://astro.ucla.edu/~wright/WISE/ (accessed on 8 May 2022).
104. NASA Space Telescope Rebooted as Asteroid Hunter. CBC News. Reuters. 22 August 2013. Available online: https://www.cbc.ca/news/science/nasa-space-telescope-rebooted-as-asteroid-hunter-1.1394598 (accessed on 8 May 2022).
105. JPL. NASA's WISE Finds Earth's First Trojan Asteroid. NASA. 27 July 2011. Available online: https://www.jpl.nasa.gov/news/nasas-wise-finds-earths-first-trojan-asteroid (accessed on 8 May 2022).

106. JPL. NASA Approves Asteroid Hunting Space Telescope to Continue Development. 11 June 2021. Available online: https://www.nasa.gov/feature/nasa-approves-asteroid-hunting-space-telescope-to-continue-development (accessed on 8 May 2022).
107. Smith, M. NASA's New NEO Mission Will Substantially Reduce Time to Find Hazardous Asteroids. Space Policy Online. 2020. Available online: https://spacepolicyonline.com/news/nasas-new-neo-mission-will-substantially-reduce-time-to-find-hazardous-asteroids/ (accessed on 8 May 2022).
108. Foust, J. NASA to Develop Mission to Search for Near-Earth Asteroids. SpaceNews. 2019. Available online: https://spacenews.com/nasa-to-develop-mission-to-search-for-near-earth-asteroids/ (accessed on 8 May 2022).
109. Lunar and Planetary Science. NEO Surveyor Mission. Available online: https://neos.arizona.edu/mission/neo-surveyor-mission (accessed on 8 May 2022).
110. Mainzer, A. NEOCam: The Near-Earth Object Camera. 2nd Small Bodies Assessment Group Meeting 18–19 November 2009 Boulder, Colorado. Available online: https://web.archive.org/web/20160624000020/http://www.lpi.usra.edu/sbag/meetings/sbag2/presentations/Mainzer_SBAG2009_NEOCam.pdf (accessed on 8 May 2022).
111. NASA/Lindley Johnson. Planetary Defense Coordination Office. 2020. Available online: https://www.nsf.gov/attachments/299316/public/8_Planetary_Defense_Coordination_Office_Update-Lindley_Johnson.pdf (accessed on 8 May 2022).
112. NASA Kennedy. KSC-20160819-PH_GEB01_0024. 2016. Available online: https://www.flickr.com/photos/nasakennedy/28869645070/ (accessed on 8 May 2022).
113. NASA/JPL-Caltech. PIA17254: NEOWISE: Back to Hunt More Asteroids (Artist Concept). 2013. Available online: https://photojournal.jpl.nasa.gov/catalog/PIA17254 (accessed on 8 May 2022).
114. NASA/JPL-Caltech. NEOCam Telescope Artist Concept. 2012. Available online: https://en.wikipedia.org/wiki/File:NEOCam_telescope_artist_concept,_NASA_JPL_Caltech.jpg (accessed on 8 May 2022).
115. Williams, M. What is the Asteroid Belt? Universe Today. 23 August 2015. Available online: https://www.universetoday.com/32856/asteroid-belt/ (accessed on 8 May 2022).
116. JPL Solar System Dynamics. JPL Small-Body Database Browser: 1 Ceres. Available online: https://ssd.jpl.nasa.gov/tools/sbdb_lookup.html#/?sstr=ceres (accessed on 8 May 2022).
117. Redd, N. Asteroid belt: Facts & information. Space.com. 4 May 2022. Available online: https://www.space.com/16105-asteroid-belt.html (accessed on 8 May 2022).
118. Edgar, R.; Artymowicz, P. Pumping of a Planetesimal Disc by a Rapidly Migrating Planet. *Mon. Not. R. Astron. Soc.* **2004**, *354*, 769–772. Available online: https://academic.oup.com/mnras/article/354/3/769/993039 (accessed on 8 May 2022). [CrossRef]
119. AllThingsSpace. Orbiting Solar System. Available online: https://sketchfab.com/sunnychen753 (accessed on 8 May 2022).
120. Granvik, M.; Morbidelli, A.; Vokrouhlický, D.; Bottke, W.F.; Nesvorný, D.; Jedicke, R. Escape of asteroids from the main belt. *Astron. Astrophys.* **2017**, *598*, A52. [CrossRef]
121. Ormö, J.; Sturkell, E.; Alwmark, C.; Melosh, J. First known terrestrial impact of a binary asteroid from a main belt breakup event. *Sci. Rep.* **2014**, *4*, 6724. [CrossRef]
122. Alwmark, C.; Alwmark-Holm, S.; Ormö, J.; Sturkell, E. Shocked quartz grains from the Målingen structure, Sweden—Evidence for a twin crater of the Lockne impact structure. *Meteorit. Planet. Sci.* **2014**, *49*, 1076–1082. [CrossRef]
123. NASA Science. Solar System Exploration—Asteroids, Comets & Meteors. Available online: https://solarsystem.nasa.gov/asteroids-comets-and-meteors/comets (accessed on 1 March 2022).
124. NASA Science. Solar System Exploration–Kuiper Belt. Available online: https://solarsystem.nasa.gov/solar-system/kuiper-belt/overview/ (accessed on 1 March 2022).
125. Delsanti, A.; Jewitt, D. The Solar System beyond the Planets (PDF). Institute for Astronomy. University of Hawaii. Available online: http://www2.ess.ucla.edu/~jewitt/papers/2006/DJ06.pdf (accessed on 2 March 2022).
126. NASA Science. Solar System Exploration—Oort Cloud. Available online: https://solarsystem.nasa.gov/solar-system/oort-cloud/overview/ (accessed on 2 March 2022).
127. Morbidelli, A. Origin and Dynamical Evolution of Comets and Their Reservoirs of Water Ammonia and Methane. *arXiv* **2005**, arXiv:0512256.
128. Clavin, W. Why Comets are Like Deep Fried Ice Cream. 10 February 2015. JPL, NASA. Available online: https://www.jpl.nasa.gov/news/why-comets-are-like-deep-fried-ice-cream (accessed on 2 March 2022).
129. Desch, S.; Jackson, A.; Noviello, J.; Anbar, A. The Chicxulub impactor: Comet or asteroid? *Astron. Geophys.* **2021**, *62*, 3.34–3.37. [CrossRef]
130. Shoemaker, E. Asteroid and comet bombardment of the Earth. *Annu. Rev. Earth Planet. Sci.* **1983**, *11*, 461–494. [CrossRef]
131. Solem, J. Density and size of Comet Shoemaker–Levy 9 deduced from a tidal breakup model. *Nature* **1994**, *370*, 349–351. [CrossRef]
132. Anderson, P. Remembering Comet Shoemaker-Levy 9's Impact on Jupiter, 23 Years Ago This Week. AmericaSpace. 17 July 2017. Available online: https://www.americaspace.com/2017/07/17/remembering-comet-shoemaker-levy-9s-impact-on-jupiter-23-years-ago-this-week/ (accessed on 8 May 2022).
133. Bruton, D. What were Some of the Effects of the Collisions? Frequently Asked Questions about the Collision of Comet Shoemaker—Levy 9 with Jupiter. Stephen F. Austin State University. 2 February 1996. Available online: http://www.physics.sfasu.edu/astro/sl9/cometfaq2.html#Q3.1 (accessed on 8 May 2022).
134. NASA Science. Solar System Exploration—Asteroids, Comets & Meteors—Oumuamua. Available online: https://solarsystem.nasa.gov/asteroids-comets-and-meteors/comets/oumuamua/ (accessed on 2 March 2022).

135. Meech, K.J.; Weryk, R.; Micheli, M.; Kleyna, J.T.; Hainaut, O.R.; Jedicke, R.; Wainscoat, R.J.; Chambers, K.C.; Keane, J.V.; Petric, A.; et al. A brief visit from a red and extremely elongated interstellar asteroid. *Nature* **2017**, *552*, 378–381. [CrossRef]
136. Bialy, S.; Loeb, A. Could Solar Radiation Pressure Explain 'Oumuamua's Peculiar Acceleration? *Astrophys. J. Lett.* **2018**, *868*, L1. [CrossRef]
137. JPL. NEO Basics. Available online: https://cneos.jpl.nasa.gov/about/basics.html (accessed on 2 March 2022).
138. JPL. Discovery Statistics. Available online: https://cneos.jpl.nasa.gov/stats/totals.html (accessed on 2 March 2022).
139. JPL. NEO Basics, NEO Groups. Available online: https://cneos.jpl.nasa.gov/about/neo_groups.html (accessed on 2 March 2022).
140. NASA. Asteroid Fast Facts. 31 March 2014. Available online: https://www.nasa.gov/mission_pages/asteroids/overview/fastfacts.html (accessed on 8 May 2022).
141. Asher, D.J.; Bailey, M.; Emel'Yanenko, V.; Napier, W. Earth in the cosmic shooting gallery. *Observatory* **2005**, *125*, 319–322.
142. Tricarico, P. The near-Earth asteroid population from two decades of observations. *Icarus* **2017**, *284*, 416–423. [CrossRef]
143. JPL. NASA's WISE Mission Finds Lost Asteroid Family Members. Available online: https://www.nasa.gov/centers/jpl/news/neowise20130528.html (accessed on 22 March 2022).
144. JPL. Planetary Defense Conference Exercise—2021. Available online: https://cneos.jpl.nasa.gov/pd/cs/pdc21/ (accessed on 2 March 2022).
145. The European Space Agency. Why the Infrared? Available online: https://www.esa.int/Science_Exploration/Space_Science/Herschel/Why_the_infrared (accessed on 8 May 2022).
146. Han, Y.; Zhang, A. Cryogenic technology for infrared detection in space. *Sci. Rep.* **2022**, *12*, 2349. [CrossRef]
147. JPL. Planetary Radar Observes 1000th Near-Earth Asteroid Since 1968. Available online: https://www.jpl.nasa.gov/news/planetary-radar-observes-1000th-near-earth-asteroid-since-1968 (accessed on 8 May 2022).
148. Tang, A.; Drouin, B.; Kim, Y.; Virbila, G.; Chang, M.-C.F. 95–105 GHz 352 mW All-Silicon Cavity-Coupled Pulsed Echo Rotational Spectroscopy System in 65 nm CMOS. *IEEE Trans. Terahertz Sci. Technol.* **2017**, *7*, 244–249. [CrossRef]
149. Nemchick, D.J.; Hakopian, H.; Drouin, B.J.; Tang, A.J.; Alonso-delPino, M.; Chattopadhyay, G.; Chang, M.C.F. 180-GHz Pulsed CMOS Transmitter for Molecular Sensing. *IEEE Trans. Terahertz Sci. Technol.* **2021**, *11*, 469–476. [CrossRef]
150. Bus, S.; Binzel, R. Phase II of the Small Main-Belt Asteroid Spectroscopic Survey. A Feature-Based Taxonomy. *Icarus* **2002**, *158*, 146–177. [CrossRef]
151. Roth, L.; Saur, J.; Retherford, K.D.; Strobel, D.F.; Feldman, P.D.; McGrath, M.A.; Nimmo, F. Transient water vapor at Europa's south pole. *Science* **2014**, *343*, 171–174. [CrossRef] [PubMed]
152. Stofan, E.R.; Elachi, C.; Lunine, J.I.; Lorenz, R.D.; Stiles, B.; Mitchell, K.L.; Ostro, S.; Soderblom, L.; Wood, C.; Zebker, H.; et al. The lakes of Titan. *Nature* **2007**, *445*, 61–64. [CrossRef] [PubMed]
153. Canavan, G.; Solem, J. Interception of near-Earth objects. *Mercury* **1992**, *21*, 107–109.
154. Hall, C.; Ross, I. Dynamics and control problems in the deflection of near-Earth objects. *Adv. Astronaut. Sci. Astrodyn.* **1997**, *97*, 613–631.
155. NASA. Asteroid Redirect Mission Planetary Defense Demonstration. 2015. Available online: http://www.nasa.gov/content/asteroid-redirect-mission-planetary-defense-demonstration/ (accessed on 28 May 2022).
156. Sergv22. Ring Array Asteroid.Gif. 2020. Available online: https://commons.wikimedia.org/wiki/File:Ring_array_asteroid.gif (accessed on 28 May 2022).
157. NASA/Johns Hopkins APL. Infographic Showing the Effect of DART's Impact on the Orbit of Didymos B while Deployment of Italian LICIACube. July 2020. Available online: https://dart.jhuapl.edu/Gallery/media/graphics/lg/DART-infographic_v4.jpg (accessed on 28 May 2022).
158. NASA/Marshall Space Flight Center. Illustration Showing NEA Scout with the Solar Sail Deployed as It Flies by Its Asteroid Destination. 2021. Available online: https://www.nasa.gov/sites/default/files/thumbnails/image/nea-scout-concept-art-high-res.jpg (accessed on 28 May 2022).
159. Coppinger, R. NASA plans 'Armageddon' spacecraft to blast asteroid. *Flightglobal* **2007**. Available online: https://web.archive.org/web/20110905041237/http://www.flightglobal.com/articles/2007/08/03/215924/nasa-plans-armageddon-spacecraft-to-blast-asteroid.html (accessed on 28 May 2022).
160. Messier, D. Nuking Dangerous Asteroids might be the Best Protection, Expert Says. 29 May 2013. Available online: http://www.space.com/21333-asteroid-nuke-spacecraft-mission.html (accessed on 28 May 2022).
161. Wie, B.; Barbee, B.; Pitz, A.; Kaplinger, B.; Hawkins, M.; Winkler, T.; Premaratne, P.; Wagner, S.; Vardaxis, G.; Lyzhoft, J.; et al. *An Innovative Solution to NASAs NEO Impact Threat Mitigation Grand Challenge and Flight Validation Mission Architecture Development*; NIAC Phase II Final Report; NASA Innovative Advanced Concepts Phase II Study; NASA: Washington, DC, USA, 2014.
162. Nuckolls, J. *Proceedings of the Planetary Defense Workshop, Lawrence Livermore National Laboratory, California, 22–26 May 1995*; Lawrence Livermore National Lab. (LLNL): Livermore, CA, USA, 1995.
163. CORDIS of European Commission. Science and Technology for Near-Earth Object Impact Prevention. Available online: https://cordis.europa.eu/project/id/640351/reporting (accessed on 8 May 2022).
164. Rivkin, A.S.; Chabot, N.L.; Stickle, A.M.; Thomas, C.A.; Richardson, D.C.; Barnouin, O.; Fahnestock, E.G.; Ernst, C.M.; Cheng, A.F.; Hirabayashi, M.; et al. The Double Asteroid Redirection Test (DART): Planetary Defense Investigations and Requirements. *Planet. Sci. J.* **2021**, *2*, 173. [CrossRef]

165. NASA. Near-Earth Object Survey and Deflection Analysis of Alternatives. Report to Congress. 2007. Available online: https://web.archive.org/web/20160303220543/http://www.nasa.gov/pdf/171331main_NEO_report_march07.pdf (accessed on 8 May 2022).
166. Melosh, H.; Nemchinov, I. Solar asteroid diversion. *Nature* **1993**, *366*, 21–22. [CrossRef]
167. Vasylyev, V. Deflection of hazardous near-Earth objects by high concentrated sunlight and adequate design of optical collector. *Earth Moon Planets* **2013**, *110*, 67–79. [CrossRef]
168. Kelley, J. Preparing for Planetary Defense: Detection and Interception of Asteroids on Collision Course with Earth. *SPACECAST* **2020**, *1*, 1992. Available online: https://apps.dtic.mil/sti/citations/ADA295142 (accessed on 8 May 2022).
169. Hughes, G.B.; Lubin, P.; Bible, J.J.; Bublitz, J.; Arriola, J.; Motta, C.; Suen, J.; Johansson, I.; Riley, J.; Sarvian, N.; et al. DE-STAR: Phased-array laser technology for planetary defense and other scientific purposes. In *Nanophotonics and Macrophotonics for Space Environments VII*; SPIE: Bellingham, DC, USA, 2013; Volume 8876. [CrossRef]
170. Bombardelli, C.; Pelaez, J. Ion beam shepherd for contactless space debris removal. *J. Guid. Control Dyn.* **2011**, *34*, 916–920. [CrossRef]
171. Fargion, D. Asteroid Deflection: How, Where and When? *arXiv* **2007**, arXiv:0705.1805.
172. Durda, D. The solar system beckons with resources unimaginable on Earth. *Ad Astra* **2006**, *18*. Available online: https://web.archive.org/web/20170721141759/http://www.nss.org/adastra/volume18/durda.html (accessed on 8 May 2022).
173. Sagan, C. *Pale Blue Dot: A Vision of the Human Future in Space*; Random House Digital, Inc.: New York, NY, USA, 1997.
174. United Nations Office for Disarmament Affairs. Treaty on the Non-Proliferation of Nuclear Weapons (NPT). 1968. Available online: https://www.un.org/disarmament/wmd/nuclear/npt/ (accessed on 9 May 2022).
175. United Nations Office for Disarmament Affairs. Treaty on Principles Governing the Activities of States in the Exploration and Use of Outer Space, including the Moon and Other Celestial Bodies. 10 October 1967. Available online: https://treaties.unoda.org/t/outer_space (accessed on 9 May 2022).
176. Guan, D.; Wang, D.; Hallegatte, S.; Davis, S.J.; Huo, J.; Li, S.; Bai, Y.; Lei, T.; Xue, Q.; Coffman, D.M.; et al. Global supply-chain effects of COVID-19 control measures. *Nat. Hum. Behav.* **2020**, *4*, 577–587. [CrossRef]